Neuron
Article

Plum, an Immunoglobulin Superfamily Protein, Regulates Axon Pruning by Facilitating TGF-β Signaling

Xiaomeng M. Yu,[1,4] Itai Gutman,[3,4] Timothy J. Mosca,[1,4] Tal Iram,[3] Engin Özkan,[2] K. Christopher Garcia,[2] Liqun Luo,[1,*] and Oren Schuldiner[3,*]
[1]Department of Biology
[2]Department of Molecular and Cellular Physiology
Howard Hughes Medical Institute, Stanford University School of Medicine, Stanford, CA 94303, USA
[3]Department of Molecular Cell Biology, Weizmann Institute of Sciences, Rehovot 76100, Israel
[4]These authors contributed equally to this work
*Correspondence: lluo@stanford.edu (L.L.), oren.schuldiner@weizmann.ac.il (O.S.)
http://dx.doi.org/10.1016/j.neuron.2013.03.004

SUMMARY

Axon pruning during development is essential for proper wiring of the mature nervous system, but its regulation remains poorly understood. We have identified an immunoglobulin superfamily (IgSF) transmembrane protein, Plum, that is cell autonomously required for axon pruning of mushroom body (MB) γ neurons and for ectopic synapse refinement at the developing neuromuscular junction in *Drosophila*. Plum promotes MB γ neuron axon pruning by regulating the expression of Ecdysone Receptor-B1, a key initiator of axon pruning. Genetic analyses indicate that Plum acts to facilitate signaling of Myoglianin, a glial-derived TGF-β, on MB γ neurons upstream of the type-I TGF-β receptor Baboon. Myoglianin, Baboon, and Ecdysone Receptor-B1 are also required for neuromuscular junction ectopic synapse refinement. Our study highlights both IgSF proteins and TGF-β facilitation as key promoters of developmental axon elimination and demonstrates a mechanistic conservation between MB axon pruning during metamorphosis and the refinement of ectopic larval neuromuscular connections.

INTRODUCTION

Neuronal remodeling is widely used for the maturation and refinement of neural circuits during the development of both vertebrate and invertebrate nervous systems (Luo and O'Leary, 2005). Often, neurons first extend exuberant branches and later remove inappropriate ones through a highly regulated pruning process. Developmental axon pruning can take place by several distinct mechanisms. In distal-to-proximal retraction (Liu et al., 2005; Portera-Cailliau et al., 2005), axonal components are retrieved by the retracting axon. In axosome shedding (Bishop et al., 2004), retracting axons discard axonal debris that are continuously engulfed by nearby cells. In localized degeneration (Watts et al., 2003), spatially defined segments of axons break into pieces that are later engulfed by surrounding glial cells. Such examples of degenerative developmental axon pruning share molecular and mechanistic similarities with axon degeneration following nerve injury and "dying back" neurodegenerative diseases (Hoopfer et al., 2006; Luo and O'Leary, 2005; Raff et al., 2002). Thus, understanding developmental pruning can provide a deeper and broader insight into axon fragmentation and elimination during development, neurodegenerative disease, and after injury.

The nervous system of *Drosophila melanogaster* undergoes massive remodeling during metamorphosis between the larval and adult stages (Truman, 1990). During this process, many central and peripheral neurons eliminate specific connections, while keeping others intact. Subsequently, they extend new axons and dendrites to form adult-specific connections (Kantor and Kolodkin, 2003; Luo and O'Leary, 2005). *Drosophila* mushroom body (MB) γ neurons have emerged as an excellent model system to study the molecular mechanisms of remodeling, as they undergo highly stereotyped axon and dendrite pruning during metamorphosis (Figure 1A). During the larval stages, γ neurons project bifurcating axons to both the medial and dorsal lobes of the MB. In early pupae, γ neurons completely prune their dendrites, along with the dorsal and medial axonal branches, up to a specific and stereotyped location. Later during development, γ neurons re-extend their axons to an adult-specific medial lobe (Lee et al., 1999; Watts et al., 2003).

MB γ neuron pruning is controlled by both intrinsic and extrinsic factors. The cell-autonomous activation of the steroid hormone Ecdysone Receptor-B1 (EcR-B1) and its coreceptor Ultraspiracle (Usp) is essential for initiating axon pruning (Lee et al., 2000). EcR-B1 is specifically expressed in γ neurons, but not in other MB neurons that do not undergo pruning. EcR-B1 expression in γ neurons is regulated by the TGF-β receptor Baboon (Babo; Zheng et al., 2003), which is activated by the glial-derived TGF-β ligand, Myoglianin (Myo; Awasaki et al., 2011). EcR-B1 expression is also regulated by a postmitotic function of the cohesin complex (Schuldiner et al., 2008) and by the nuclear receptors Hr39 and Ftz-f1 (Boulanger et al.,

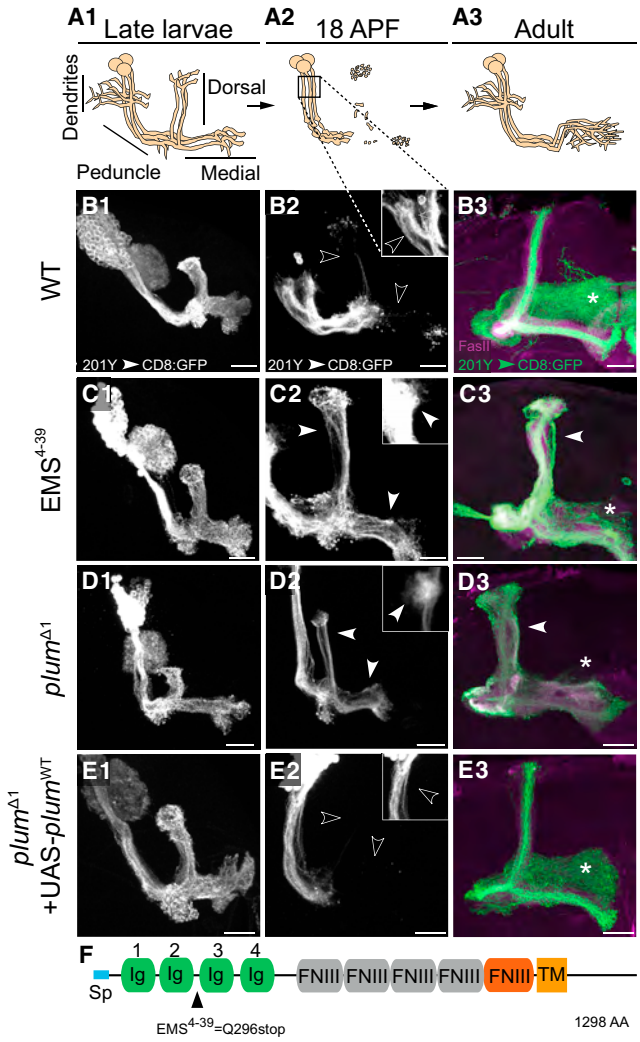

Figure 1. Plum Is an IgSF Member Required for Axon Pruning of MB γ Neurons

(A) Scheme of developmental pruning of MB γ neurons. During embryonic and larval life, each γ neuron extends a single process that branches near the cell body to form dendrites and continues as an axon peduncle that bifurcates to form a dorsal and a medial branch (A_1). Both axonal branches, as well as dendrites, are pruned by 18 hr after puparium formation (APF), whereas the peduncle remains intact (A_2). Subsequently, γ neurons extend axons only medially to adult-specific lobes (A_3). Square in (A_2) marks the location of dendrites that are shown in the insets of (B_2)–(E_2).

(B–E) Confocal Z-projections of (B) WT (n = 20), (C) EMS$^{4-39}$ (n = 13), (D) *plum*$^{\Delta 1}$ (n = 13), and (E) *plum*$^{\Delta 1}$ additionally expressing a Plum^{WT} transgene (UAS-*plum*^{WT}; n = 13) MB neuroblast clones. MARCM clones are labeled with 201Y-GAL4-driven mCD8::GFP at (B_1–E_1) the third-instar larval stage, (B_2–E_2) 18 hr APF, and (B_3–E_3) in adults. Solid arrowheads indicate unpruned γ axons and dendrites, while open arrowheads indicate fragmented γ axons and dendrites. Asterisks indicate the distal tip of the adult γ lobe. White or green, 201Y-GAL4-driven mCD8::GFP; magenta, FasII. Scale bars, 20 μm. (F) Domain structure of the Plum protein with EMS$^{4-39}$ depicted (Q296stop). Blue, signal peptide (Sp); green, immunoglobulin (Ig) domains; gray, putative Fibronectin-III (FNIII) domains; red, FNIII domain; and orange, transmembrane domain (TM).

See also Figure S1.

2011). While the apoptotic machinery (including the caspase *Dronc*) is required for dendrite pruning of sensory neurons (Kuo et al., 2006; Williams et al., 2006), it does not appear to be required for dendrite or axon pruning of MB neurons (Watts et al., 2003; E. Hoopfer, L.L., and O.S., unpublished data). Following fragmentation, the neuronal debris is engulfed by nearby glia (Awasaki and Ito, 2004; Watts et al., 2004) in a *draper* (*ced-1* homolog)-dependent manner (Awasaki et al., 2006; Hoopfer et al., 2006) and degraded via an endosomal-lysosomal pathway (Watts et al., 2004).

Despite significant progress in the past decade, our understanding of developmental axon pruning is far from complete. Specifically, very little is known about the nature of cell-cell communication during axon pruning. Through a forward genetic screen, we identified Plum, an immunoglobulin superfamily (IgSF) protein that functions at the cell surface of MB γ neurons and is cell autonomously required for axon pruning. Genetic analyses revealed that Plum promotes pruning by regulating the expression of EcR-B1. Our data suggest that Plum achieves this regulation by facilitating the signal via canonical TGF-β type I/II receptors in response to a glial-derived TGF-β ligand, Myoglianin. Our results also demonstrate molecular conservation in the signaling events that occur in both remodeling of MB neurons during metamorphosis and the refinement of ectopic terminals at the larval neuromuscular junction (NMJ). These underlying similarities indicate Plum as a general regulator of developmental axon elimination.

RESULTS

Plum Is an Immunoglobulin Superfamily Protein Required for Axon Pruning

To identify molecules that are required for MB γ neuron pruning, we performed a forward genetic screen using the mosaic analysis with a repressible cell marker technique (MARCM; Lee and Luo, 1999). In this screen, mutations were induced by the chemical mutagen EMS, and phenotypes were examined in MARCM clones (see the Experimental Procedures). To visualize MB γ neurons, we generated neuroblast clones that express a membrane-bound GFP (mCD8::GFP) driven by the 201Y-GAL4 driver (Yang et al., 1995), which is expressed in γ neurons during the larval and early pupal stages and in both γ and a subset of the later-born α/β neurons at the adult stage (Schuldiner et al., 2008). We found a mutant, EMS$^{4-39}$, which caused a severe pruning defect (compare Figure 1C with Figure 1B). In wild-type (WT) brains, the dorsal and medial γ-axon branches, as well as dendrites, were completely pruned at 18 hr after puparium formation (APF; Figure 1A_2, open arrowheads in Figure 1B_2). In contrast, γ neurons homozygous for EMS$^{4-39}$ retained these axonal branches as well as their dendrites (see insets for a focus on dendrites, as outlined by the box in Figure 1A_2), indicating a failure in pruning (solid arrowheads in Figure 1C_2) of both dendrites and axons. Because of the relative technical ease, we have focused our studies below on axon pruning. These unpruned axons persisted into the adult stage as dorsal branches that lie outside the α-lobe (solid arrowhead in Figure 1C_3). As a consequence, very few mutant γ neurons innervate the adult γ-lobe (compare asterisks in Figures 1C_3 and

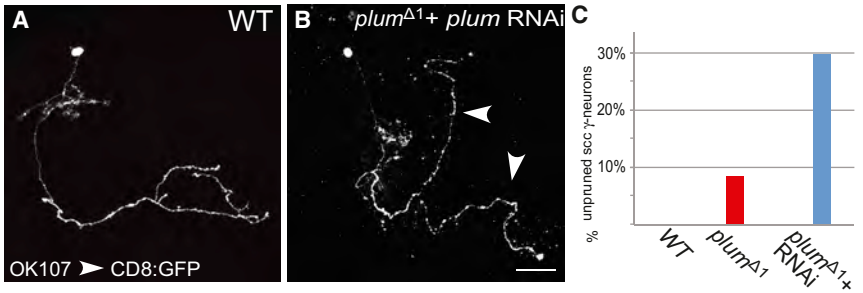

Figure 2. Plum Is Cell Autonomously Required for Axon Pruning of MB γ Neurons

(A) Confocal Z-projection of a WT single cell clone.

(B) Confocal Z-projection of a single cell clone homozygous for *plum*$^{\Delta 1}$ additionally expressing a *plum* RNAi (UAS-*plum*^{RNAi}) transgene. In both (A) and (B), γ single cell clones are labeled by OK107-GAL4 driving the expression of mCD8::GFP. Arrowheads in (B) indicate unpruned γ axon branches that persist into the adult stage. Scale bar, 20 μm.

(C) Quantification of pruning defects in single cell clones.

1B_3). This pruning defect is unlikely to be caused by a secondary effect due to impaired axon growth or guidance defects, as EMS$^{4\text{-}39}$ mutant γ neuron clones appeared normal at the third-instar larval stage, prior to the onset of axon pruning (compare Figures 1C_1 to 1B_1).

Combining SNP and deficiency mapping (see the Experimental Procedures), we identified the EMS$^{4\text{-}39}$ mutation as a nonsense mutation (Q296Stop; see Figure 1F; see Figure S1 available online) in a gene—*CG6490*. We named the gene *plum*, because mutant γ neurons do not "prune." We also generated two small deficiencies—*plum*$^{\Delta 1}$ and *plum*$^{\Delta 2}$—using *cis*-FRT mediated recombination (Figure S1; see the Experimental Procedures), which confirmed that MB MARCM clones lacking *plum* exhibited severe pruning defects (compare asterisks in Figures 1D_3 to 1B_3, results shown for *plum*$^{\Delta 1}$). We used *plum*$^{\Delta 1}$ for most of our subsequent experiments.

plum encodes a transmembrane, immunoglobulin superfamily (IgSF) protein (Figure 1F). Domain analysis of the Plum protein revealed four immunoglobulin (Ig) domains, one Fibronectin III (FNIII) domain predicted by the SMART algorithm (http://smart.embl-heidelberg.de/), and four additional putative FNIII domains (Figure 1F). Expression of an epitope-tagged, full-length *plum* transgene (UAS-*plum*^{WT}*:Flag*; hereafter termed Plum^{WT}) within *plum*$^{\Delta 1}$ MB MARCM neuroblast clones fully rescued their pruning defect (Figure 1E). Thus, we conclude that Plum is an IgSF protein that plays an essential role during MB γ neuron pruning.

Plum Is Cell Autonomously Required in Postmitotic γ Neurons for Axon Pruning

To determine whether Plum is required cell autonomously to regulate pruning, we generated MB γ neuron MARCM single cell clones (SCCs) homozygous for *plum*$^{\Delta 1}$ in otherwise heterozygous brains (Figures 2A and 2B). We found that 8.5% of the *plum*$^{\Delta 1}$ SCCs (n = 47) (Figure 2C, red bar) retained their larval-specific dorsal axon branches into the adult stage, whereas all WT γ neurons pruned these branches (Figure 2A). This low percentage of unpruned SCCs might be caused by perdurance of Plum RNA or protein in SCCs (for a more detailed explanation of perdurance, see the Experimental Procedures). Indeed, expressing Plum RNAi within mutant single cell clones raised the percentage of unpruned SCCs to 30% (n = 115; Figure 2B, quantified in Figure 2C, blue bar). These results indicate that Plum is cell autonomously required in γ neurons for their axon pruning.

Two additional lines of evidence suggest that Plum functions in postmitotic neurons. First, defects in SCCs resulted from lack of Plum protein only in postmitotic γ neurons. Second, in our rescue experiment (Figure 1E), we used a driver that, in the MB, is only expressed in postmitotic neurons (201Y-GAL4; Schuldiner et al., 2008) to drive the expression of Plum^{WT} in mutant neuroblast clones (Figure 1E). Because GAL4 expression turned on only after the last round of cell division that produces the neuron, these results, along with pruning defects in single cell clones, indicate that Plum functions cell autonomously in postmitotic γ neurons to promote axon pruning.

The Extracellular Domain of Plum Is Required for Axon Pruning

IgSF proteins are implicated in diverse steps of brain development, including neuronal migration, axon pathfinding, target recognition, synapse formation, and in the maintenance and function of adult neuronal networks (Rougon and Hobert, 2003; Vogel et al., 2003). In all cases examined, IgSF proteins mediate cell-cell interactions through their Ig and FNIII domains (Brümmendorf and Rathjen, 1996). If Plum functions in cell-cell communication, one or both of these domains should be essential for its function. To assess the role of the Ig domains in the function of Plum during pruning, we performed in vivo structure-function analyses. We generated a series of epitope-tagged UAS-*plum* transgenes in which specific domains were deleted (UAS-*plumΔdomain:Flag* are abbreviated as Plum$^{\Delta domain}$) and tested their ability to rescue γ neuron pruning defects when expressed within *plum*$^{\Delta 1}$ MARCM neuroblast clones.

We found that deletion of any or all of the first three Ig domains (Figure 3A; results for single deletions not shown) did not affect the rescue abilities of the transgenes (Figure 3F), indicating that Ig domains 1–3 are not required for Plum's function during pruning. In contrast, deletion of all four Ig domains (Plum$^{\Delta Ig1\text{-}4}$) nearly abolished the rescue ability of the transgene (Figures 3B and 3F). In addition, deletion of Ig4 domain (Plum$^{\Delta Ig4}$) partially reduced the rescue ability of that transgene (Figures 3C and 3F). Deletion of these domains resulted in some changes to expression and localization (Figure S2), but these did not correlate with their rescue ability. Our results therefore demonstrate the importance of Plum's extracellular domain, and specifically the four Ig domains as a whole, in mediating axon pruning.

Many IgSF proteins, such as *Drosophila* Fasciclin II, Neuroglian, and DSCAM, execute their functions through a *trans*-homophilic binding mechanism (Agarwala et al., 2000; Islam

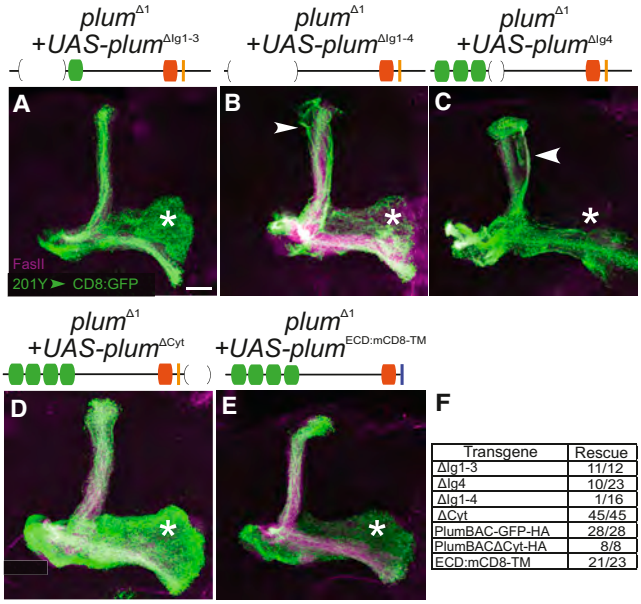

Transgene	Rescue
ΔIg1-3	11/12
ΔIg4	10/23
ΔIg1-4	1/16
ΔCyt	45/45
PlumBAC-GFP-HA	28/28
PlumBACΔCyt-HA	8/8
ECD:mCD8-TM	21/23

Figure 3. Structure-Function Analysis of Plum

(A–E) Confocal Z-projections of *plum*$^{\Delta 1}$ MB MARCM neuroblast clones additionally expressing (A) UAS-*plum*$^{\Delta Ig1\text{-}3}$ (n = 12), (B) UAS-*plum*$^{\Delta Ig1\text{-}4}$ (n = 16), (C) UAS-*plum*$^{\Delta Ig4}$ (n = 23), (D) UAS-*plum*$^{\Delta Cyt}$ (n = 45), and (E) UAS-*plum*$^{ECD:CD8\text{-}TM}$ (n = 23). Whereas expression of Plum$^{\Delta Ig1\text{-}3}$ (A), Plum$^{\Delta Cyt}$ (D), or Plum$^{ECD:CD8\text{-}TM}$ (E) rescued the pruning defect, expression of Plum$^{\Delta Ig1\text{-}4}$ (B) or Plum$^{\Delta Ig4}$ (C) did not.

(F) Summary of Plum truncations and their ability to rescue the pruning defects of *plum*$^{\Delta 1}$ MB MARCM neuroblast clones. PlumBAC-GFP:HA and PlumBACΔCyt:HA were expressed under the control of the endogenous promoter (see Figure S4), while 201Y-GAL4 drove expression of the other transgenes. Plum-predicted domains are depicted as shown in Figure 1F, with brackets representing the deleted domains; the mCD8 transmembrane domain is represented by a blue line. Green, 201Y-GAL4-driven mCD8::GFP; magenta, FasII; and an asterisk marks adult-specific γ-lobe. Scale bar, 20 μm.

See also Figures S2 and S3.

et al., 2004; Schuster et al., 1996). We explored the formation of Plum *trans*-homophilic interaction using a *Drosophila* S2 cell aggregation assay. We found that expression of Plum promoted S2 cell aggregation (Figure S3). However, Plum-mediated *trans*-homophilic interaction required Ig domains 1–3 (Figure S3), which were not required in vivo to promote pruning (Figure 3). These data suggest that, in vivo, *trans*-homophilic interaction is not required for Plum's function in MB γ axon pruning. Therefore, Plum likely interacts with a heterophilic ligand to regulate MB γ neuron axon pruning.

The Cytoplasmic Domain of Plum Is Not Required for Axon Pruning

The cell-autonomous requirement for *plum* in MB γ neurons suggests that it functions genetically as a receptor. We therefore tested the requirement of the cytoplasmic domain for Plum's function. To our surprise, expressing a Plum transgene lacking its cytoplasmic domain (Plum$^{\Delta Cyt}$) was sufficient to rescue the pruning defect of *plum*$^{\Delta 1}$ MB γ neurons (Figures 3D and 3F). To confirm that this was not an artifact due to overexpression of the transgene, we generated *plum*$^{\Delta 1}$ homozygous flies expressing *plum* transgenes with or without its cytoplasmic domain under the control of its own promoter using bacterial artificial chromosome (BAC) recombineering (PlumBAC-GFP:HA and PlumBACΔCyt:HA, respectively; Figure S4). We found that both BAC transgenes rescued the mutant phenotype of *plum*$^{\Delta 1}$ neuroblast clones in a similar manner (Figure 3F), confirming that the cytoplasmic domain is not required for pruning.

To exclude the possibility that the Plum$^{\Delta Cyt}$ transgene can elicit a signal to promote pruning by the transmembrane domain or the residual nine remaining cytoplasmic amino acids, we generated another transgene, encoding for the Plum extracellular domain fused to the mouse CD8 transmembrane domain (UAS-*plum-ECD:*CD8-*TM:Flag*; Plum$^{ECD:CD8\text{-}TM}$). We found that expression of the Plum$^{ECD:CD8\text{-}TM}$ transgene also rescued the pruning defect in *plum*$^{\Delta 1}$ MB γ neurons (Figures 3E and 3F). Thus, although Plum functions cell autonomously, neither its cytoplasmic nor its transmembrane domain conveys the pruning signal. These data suggest that Plum transduces signals via the activity of another receptor to direct γ neuron axon pruning.

Despite Panneural Expression, Plum Is Required Only within MB γ Neurons for Their Pruning

To gain insight into Plum's function in cellular communication, we generated polyclonal antibodies against the extracellular domain of Plum and examined its endogenous localization in the central brain during development. At 6 hr APF, a developmental time point at which MB γ neuron pruning has already begun (Watts et al., 2003), Plum was broadly expressed in the neuropil (Figures 4A–4C). The staining was completely eliminated in homozygous *plum*$^{\Delta 1}$ animals (Figures 4D–4F), demonstrating the specificity of the antibody. Within the MB, Plum was expressed at a low level and was localized to both axons and dendrites (yellow outlines in Figures 4B and 4C). Plum was detected in very low levels at the cell bodies (white outline in Figure 4C). Interestingly, Plum was expressed at a higher level in the neuropil outside the MB (Figure 4B, outside the yellow outline). This widespread expression was also confirmed by the localization of a GFP-tagged genomic *plum* transgene (PlumBAC-GFP:HA; Figure S4B). Plum staining in late third-instar larval (Figures 4G′, 4H′, and 4I′) and 0 hr APF pupal brains (data not shown) appeared similar to 6 hr APF.

To determine whether the non-MB Plum staining originates from neurons or glia, we knocked down Plum's expression specifically in both or either one of these cells by using GAL4 drivers that are ubiquitous (*actin5c-GAL4*), panneuronal (C155-GAL4), or panglial (*repo-GAL4*) to drive the expression of a UAS-*plumRNAi* transgene. We found that ubiquitous or panneuronal RNAi knockdown of Plum eliminated the antibody staining (Figures 4G and 4H), while panglial knockdown did not (Figure 4I). Consistently, using a GAL4-independent MB fluorescence reporter (Figures S4C–S4L), we found that ubiquitous and panneuronal, but not glial, knockdown of Plum caused strong pruning defects (n = 20 for each genotype; data not shown). Therefore, Plum is expressed predominantly in neurons in the developing brain.

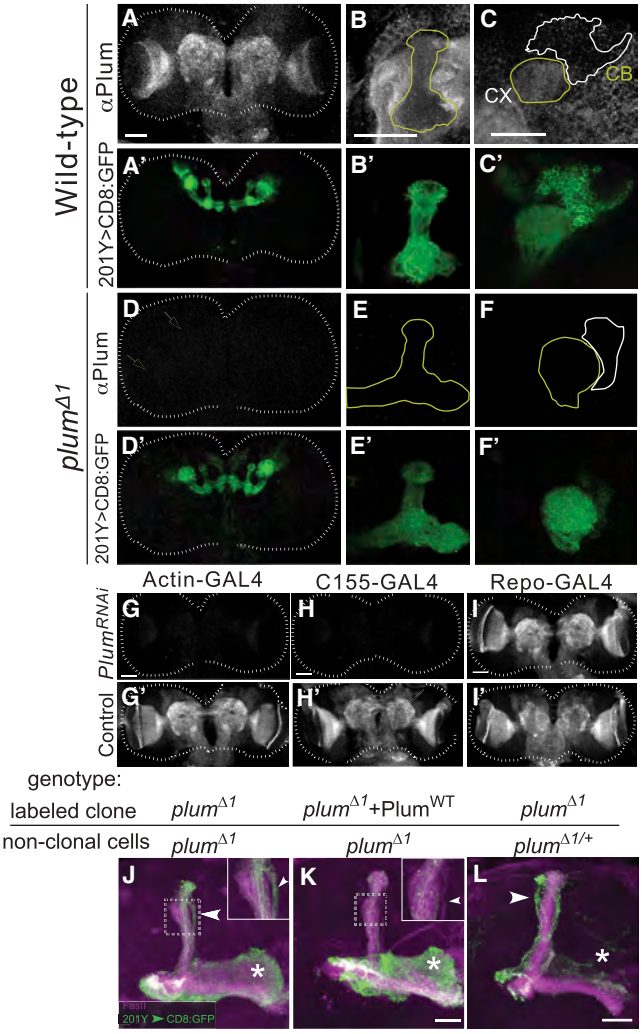

Figure 4. Despite Widespread Expression, Plum Is Required Only in MB γ Neurons for Axon Pruning

(A–F) Confocal Z-projections of (A–C) WT and (D–F) *plum*$^{\Delta 1}$ 6 hr APF brains depicting (A–F) anti-Plum staining or (A′–F′) MB structure by 201Y-GAL4-driven mCD8::GFP. (B and E) Close-up view of the MB dorsal lobe (outlined in yellow). (C and F) Close-up of the calyx (CX; outlined in yellow) and cell bodies (CB; outlined in white). Similar results were obtained by examining 15 brains from each genotype.

(G–I) Z-projections of Plum staining in third-instar larval brains that express Plum RNAi driven by (G) Actin-GAL4, (H) C155-GAL4 and (I) *repo-GAL4*. (G′)–(I′) are controls with the GAL4 transgenes alone. Scale bars in (A)–(I) are 50 μm. Similar results were obtained by examining 8–10 brains from each genotype.

(J and K) Confocal Z-projections of an MARCM-labeled MB neuroblast clone from a brain in which all cells are *plum*$^{\Delta 1}$ mutant in the absence (J) or presence (K) of an additional Plum^{WT} rescue transgene expressed within the clone. Seven out of eight clones in (J) and 1 out of 14 in (K) exhibited unpruned projections. Insets show a close-up view of the dorsal lobe. Arrowheads point to the unpruned dorsal lobe of γ axons, which fall outside the FasII staining (magenta, marker of α/β axons). Asterisks indicate adult-specific γ axons in the medial lobe.

(L) Confocal Z-projections of a *plum*$^{\Delta 1}$ MARCM neuroblast clone in an otherwise *plum*$^{\Delta 1/+}$ brain (n = 13). Compared with (J), there are more unpruned γ axons in the dorsal lobe (arrowhead) and fewer adult-specific γ axons (asterisk), indicating a much more severe pruning defect in (L). Green is mCD8::GFP; magenta is FasII staining.

Because Plum is highly expressed in the neuropil adjacent to MB axons, we tested whether it has an additional, non-cell-autonomous role in γ axon pruning. We first examined this possibility by determining whether Plum expression within γ neurons is sufficient to promote pruning. We took advantage of the fact that *plum*$^{\Delta 1}$ flies are homozygous viable and generated MARCM neuroblast clones expressing Plum^{WT} in an otherwise *plum*$^{\Delta 1}$ mutant brain. Because MB neurons are born from four identical neuroblasts (Ito et al., 1997), expression of the Plum^{WT} transgene within a MARCM clone would result in one clone of positively labeled *plum*$^{\Delta 1}$ neurons expressing Plum^{WT}, whereas the remaining three-fourths of MB neurons (as well as the rest of the brain), would be unlabeled, homozygous mutants. We found that expressing Plum^{WT} in a neuroblast clone was sufficient to rescue the pruning defect in *plum*$^{\Delta 1}$ mutant brains (Figure 4K, compared to Figure 4J), demonstrating that Plum is only required within γ neurons to promote axon pruning.

Interestingly, labeled *plum*$^{\Delta 1}$ MB neuroblast clones within homozygous mutant brains (where all cells were *plum*$^{\Delta 1}$ but only a neuroblast clone was labeled; Figure 4J) displayed markedly weaker pruning defects compared to *plum*$^{\Delta 1}$ clones within otherwise *plum* heterozygous brains (Figure 4L). In *plum*$^{\Delta 1}$ homozygous mutant brains, MB neuroblast clones displayed both unpruned dorsal larval axons as well as normal adult axons (Figure 4J, asterisk), indicating that a significant proportion of γ neurons pruned normally. By contrast, in otherwise *plum* heterozygous brains, *plum*$^{\Delta 1}$ γ neuron MARCM clones did not contain any adult medial axons (Figures 1D$_3$ and 4L, asterisk), suggesting that all γ neurons within the clone failed to prune. Indeed, a blind rank order test based on pruning severity clearly separated the two genetic conditions (Figure S5A). Because the labeled axons in both cases were of the same genotype, their phenotypic differences suggest that Plum expression outside the clone negatively regulates MB γ axon pruning. A likely interpretation is that Plum outside the MB competes for a ligand used by Plum within the MB (see the Discussion).

Plum Promotes Axon Pruning by Regulating EcR-B1 Expression

To investigate the mechanism by which Plum regulates axon pruning, we tested its relationship with other molecular pathways required for MB γ neuron axon pruning. The steroid hormone receptor EcR-B1 is a major initiator of axon pruning (Lee et al., 2000), whose expression is regulated by multiple mechanisms (see the Introduction). Remarkably, we found that Plum was also required for EcR-B1 expression, as EcR-B1 expression was absent in *plum*$^{\Delta 1}$ MARCM γ neuron clones (compare Figure 5B with Figure 5A). Transgenic expression of Plum^{WT} (Figure 5C) or Plum$^{\Delta Cyt}$ (Figure 5D) within *plum*$^{\Delta 1}$ mutant MARCM clones restored EcR-B1 expression. Interestingly, in *plum*$^{\Delta 1}$ homozygous mutant brains, where only a subset of MB γ neurons failed to prune (Figure 4J), we also observed a corresponding partial loss of EcR-B1 expression in MB γ neurons (Figure S6).

Scale bars in (J)–(L) are 20 μm. Figure S5A shows the result of a blind rank order to compare the phenotypes in Figures 3J and 3L. See also Figure S4.

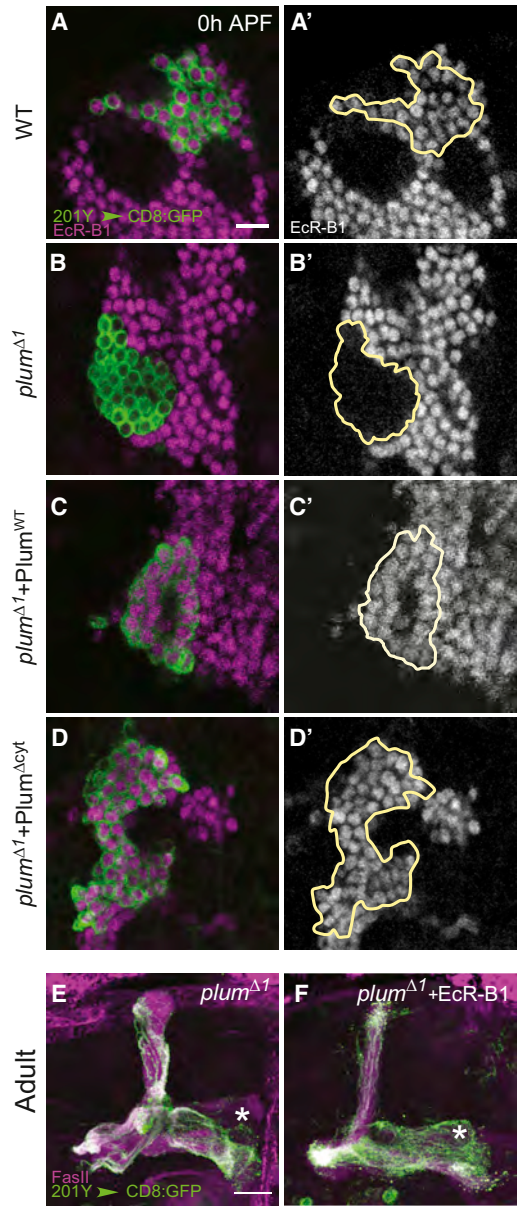

Figure 5. Plum Controls Axon Pruning by Regulating EcR-B1 Expression

(A–D) Representative single confocal sections of the cell body regions of 0 hr APF MB MARCM neuroblast clones in (A) WT (n = 6), (B) *plum*$^{\Delta 1}$ (n = 10), and (C) *plum*$^{\Delta 1}$ additionally expressing Plum^{WT} (n = 6) or (D) Plum$^{\Delta Cyt}$ (n = 5). Left panels show both MARCM clones labeled by 201Y-GAL4-driven mCD8::GFP (green) and EcR-B1 expression (magenta). Right panels show EcR-B1 expression (gray); clones are outlined. Scale bar: 10 μm. n is number of clones examined.

(E and F) Confocal Z-projections of (E) *plum*$^{\Delta 1}$ (n = 14) and (F) *plum*$^{\Delta 1}$ additionally expressing UAS-*EcR-B1* (n = 15). Green, 201Y-GAL4-driven mCD8::GFP; magenta, FasII; asterisks mark the adult-specific γ lobe. Scale bars are 20 μm. Figure S5B shows the result of a blind rank order to compare the phenotypes in Figures 4E and 4F.

See also Figure S6.

Finally, overexpression of EcR-B1 within *plum*$^{\Delta 1}$ MARCM clones largely rescued their pruning defect (compare Figure 5F with Figure 5E; see Figure S5B for a blind rank order test). These results indicate that a major function of Plum in axon pruning lies in its regulation of EcR-B1 expression.

Plum Acts Upstream of the TGF-β Receptor Baboon

The only cell-surface proteins known to be involved in MB pruning are the TGF-β receptors, Babo (type I receptor), and Wishful thinking (Wit) and Punt (type II receptors). Together, they function to upregulate the expression of EcR-B1 prior to axon pruning (Zheng et al., 2003). Given the similarity between the functions of Plum and Babo, and our finding that Plum relies on another receptor for its signaling, we hypothesized that the two may function together to regulate MB pruning.

To determine the relationship between Plum and Babo, we overexpressed UAS transgenes corresponding to each gene in a mutant MARCM clone of the other. We found that overexpression of either Babo^{WT} or constitutively active Babo (UAS-babo^{Q302D}; Brummel et al., 1999) in *plum*$^{\Delta 1}$ mutant MARCM clones rescued both EcR-B1 expression (Figures 6A and 6A′; data not shown, respectively) and the pruning defects (Figures 6B and S5C). These results indicate that upregulation of TGF-β signaling can compensate for the loss of Plum. Similarly, we also found that overexpression of a phosphomimetic active form (SmoX^{SDVD}) of dSmad2 (also known as SmoX; Gesualdi and Haerry, 2007), the factor downstream of Babo signaling, also partially rescued EcR-B1 expression (Figures 6C and 6C′) and the pruning defects (Figures 6D and S5C) of *plum*$^{\Delta 1}$ mutant MARCM clones. The converse is not true: overexpression of Plum^{WT} within *babo* MARCM γ neuron mutant clones did not rescue the loss of EcR-B1 expression (Figures 6E and 6E″) or the pruning defects (Figure 6F). These results suggest that Plum acts upstream of Babo to regulate EcR-B1 expression and axon pruning (Figure 6I).

Plum Interacts Genetically with the TGF-β Ligand Myoglianin

Because Babo receives its signal from the glial-derived Myo (Awasaki et al., 2011), we tested whether Plum also interacts with Myo. Indeed, we found strong genetic interactions between Plum and Myo in three separate experiments. First, ectopic, panglial expression of Plum$^{\Delta Cyt}$ (using *repo-GAL4*) in WT animals resulted in an axon-pruning defect (Figure 6G). This effect was dose-dependent, as higher Plum$^{\Delta Cyt}$ expression (caused by higher GAL4 activity when animals were raised at higher temperatures) resulted in stronger pruning defects (Figure 6G, compare first, second, and third columns). At the same time, reducing the endogenous *plum* gene dose also resulted in a stronger pruning defect (Figure 6G, compare fourth to first column). Interestingly, co-overexpression of Myo and Plum$^{\Delta Cyt}$ in glia partially suppressed this pruning defect (Figure 6G, compare fifth to second column). The simplest interpretation for these results is that Plum$^{\Delta Cyt}$ overexpression in glia causes a pruning defect because of Myo sequestration. Reduction of endogenous Plum exacerbated, whereas glial coexpression of Myo alleviated, this sequestration effect and thus enhanced or suppressed the pruning defect, respectively.

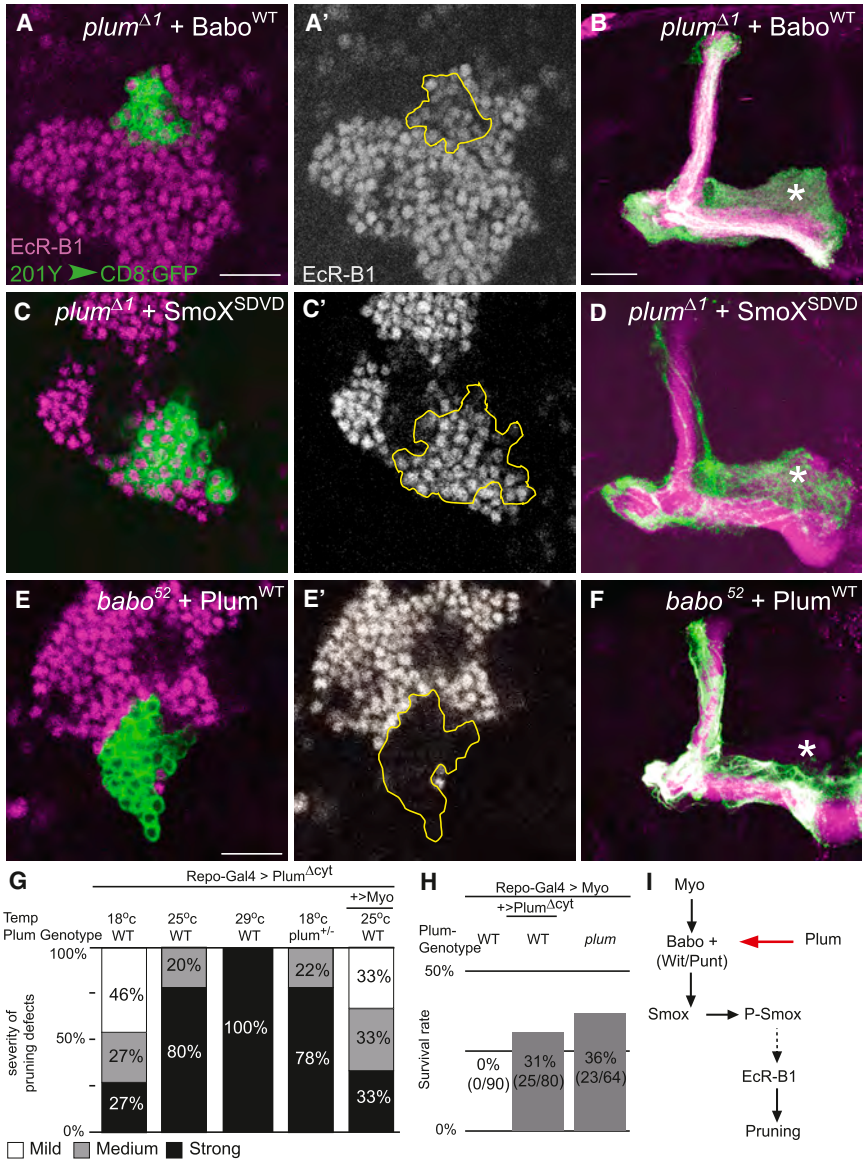

Figure 6. Plum Facilitates TGF-β Signaling

(A–F) Single confocal sections (A, C, and E) of 0 hr APF MB cell bodies or (B, D, and F) confocal Z-projections of adult MB neurons of the following genotypes: (A and B) *plum*$^{\Delta 1}$ MB MARCM neuroblast clones additionally expressing Babo^{WT} (n = 8) or (C and D) SmoX^{SDVD} (n = 11) or (E and F) *babo*^{52} neuroblast clones additionally expressing Plum^{WT} (n = 26). Green, 201Y-GAL4-driven mCD8::GFP; magenta/gray in (A), (C), and (E), EcR-B1; magenta in (B), (D), and (F), FasII; and asterisks mark the adult-specific γ lobe. Scale bars are 20 μm. Figure S5C shows the result of a blind rank order test to compare the phenotypes in Figures 5B, 5D, and 5F.

(G) Quantification of the pruning defects seen in animals of different genotypes and rearing conditions. Plum$^{\Delta Cyt}$ was overexpressed in glia in WT or *plum*$^{\Delta 1/+}$, or was coexpressed together with Myo in WT animals. Sample sizes (n) scored for each condition are (from left to right): 22, 18, 20, 32, and 25. See the Experimental Procedures for definitions of the different severity levels.

(H) Survival rates of WT or *plum*$^{\Delta 1}$ animals overexpressing Myo alone or together with Plum$^{\Delta Cyt}$ in glia (see the Experimental Procedures).

(I) Scheme of Plum integration into the TGF-β signaling pathway based on genetic data.

Plum Regulates Ectopic Motoneuron Projections at the NMJ through EcR-B1

At the mammalian neuromuscular junction (NMJ), the mature pattern of connectivity is achieved via a general process of synaptic refinement that eliminates weak connections and prevents improper ones (Nguyen and Lichtman, 1996). At the fly larval NMJ, developmental synaptic refinement also occurs to produce normal neuromuscular connectivity. While some of the mechanistic bases for refinement by synapse retraction are known (Eaton et al., 2002; Massaro et al., 2009; Pielage et al., 2005), other forms involving the prevention of off-target, ectopic contacts (Carrillo et al., 2010; Jarecki and Keshishian, 1995; Kopczynski et al., 1996) are not as well understood.

To examine whether Plum is required for normal neuromuscular connectivity, we stained the NMJs of WT and *plum* mutant third-instar larvae with antibodies to horseradish peroxidase (HRP) (Figures 7A and 7B) and quantified the number of ectopically placed connections onto muscles 6 and 7. We found that in *plum*$^{\Delta 1}$ or *plum*$^{\Delta 2}$ larvae, the frequency of improper, ectopic connections was increased nearly 6-fold (27.1% and 28.1%, respectively) over WT (4.8%) larvae (Figure 7C). Whereas the majority of these ectopic connections were made by the transverse nerve, we also observed improper connections from other motoneurons that normally innervate muscles 13, 15, and 28 (data not shown). The increased frequency of ectopic

Second, previous findings indicated that ubiquitous expression of Myo causes lethality (Awasaki et al., 2011). We found that panglial overexpression of Myo recapitulated this lethality (Figure 6H, first column); most animals died as larvae. However, coexpression of Plum$^{\Delta Cyt}$ together with Myo in glia resulted in 31% of the animals surviving to adulthood (Figure 6H, second column). This suggests that glial overexpression of Plum$^{\Delta Cyt}$ mitigates lethality by sequestering excessive Myo, which by itself is toxic.

Third, lethality caused by glial overexpression of Myo was also suppressed in homozygous *plum* mutants (Figure 6H, third column), indicating that endogenous Plum is required to transduce the Myo-derived signals that cause lethality. Because MB γ axon pruning is not essential for viability, this third experiment indicates that Plum interacts with Myo in a more general context, beyond MB axon pruning.

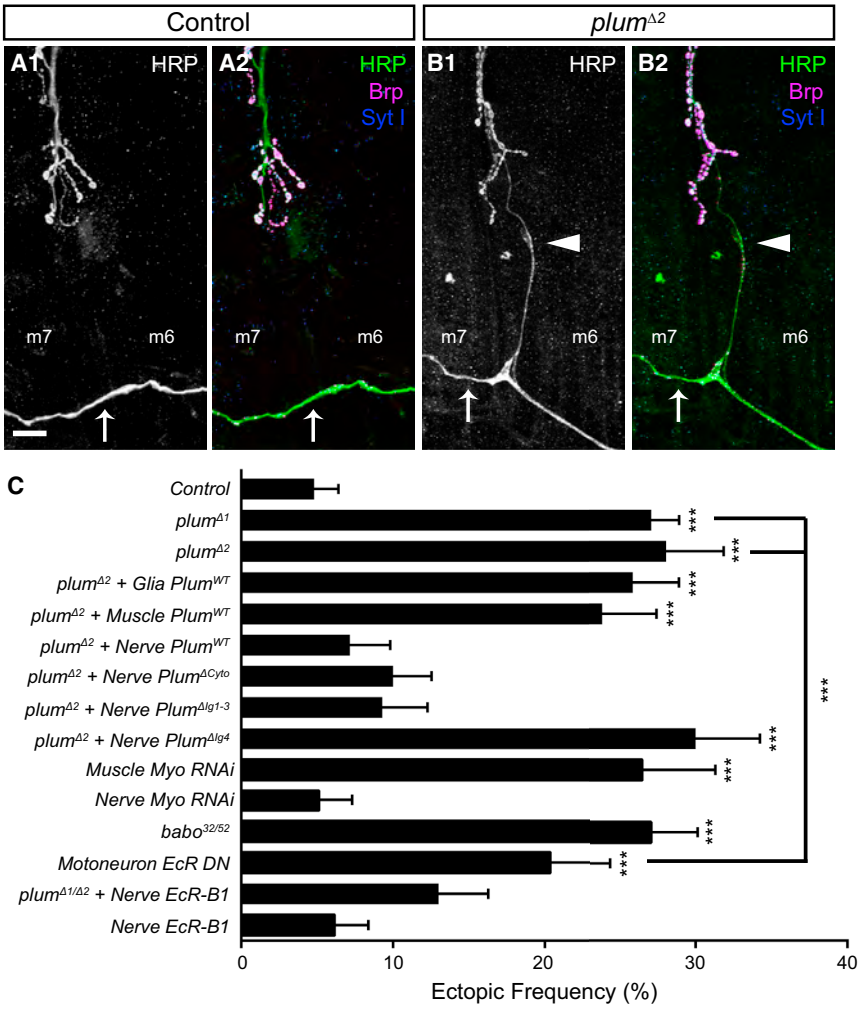

Figure 7. Neuronal *plum* and TGF-β Signaling Is Required for Refinement of Connections at the Third-Instar Neuromuscular Junction

(A) Representative confocal image of the lower portion of the neuromuscular junction (NMJ) between muscles 6 and 7 in a control third-instar larva stained with antibodies to HRP (A_1 and green in A_2), Brp (magenta), and Synaptotagmin I (blue). Under normal conditions, the transverse nerve (arrow) does not make any connections to the muscle, which is otherwise normally innervated.

(B) Representative confocal image in a $plum^{\Delta 2}$ third-instar larvae stained as in (A). Here, the transverse nerve (arrow) has made an inappropriate ectopic connection onto muscle 6 (arrowhead); this connection possesses release machinery and synaptic vesicles. Scale bar is 20 μm.

(C) Quantification (mean ± SEM) of the frequency of larval hemisegments with at least one ectopic neuromuscular projection expressed as a percentage of the total hemisegments examined in third-instar larvae with various genotypes listed on the left. In all cases, n ≥ 5 larvae and 60 hemisegments scored.

Error bars represent ± SEM. ***, $p < 0.001$. See also Figure S7.

connections was not a secondary effect of altered connectivity at normal (i.e., not ectopic) NMJs, as *plum* mutant NMJs displayed normal targeting and bouton number, as compared to WT larvae (Figures S7F–S7H).

Plum acts in neurons to regulate normal connectivity, as restoring neuronal (but not muscle or glial) expression of Plum within a $plum^{\Delta 2}$ background was sufficient to restore the number of hemisegments with ectopic connections to WT levels (Figure 7C). Moreover, neuronal knockdown of Plum using a UAS-*plum* RNAi transgene phenocopied the increase in ectopic connections seen in $plum^{\Delta 2}$ flies, whereas muscle knockdown did not (Figure S7). Therefore, Plum acts in motoneurons via a heterophilic ligand to ensure normal connectivity.

We also conducted a structure-function analysis of Plum at the NMJ, similar to the MB (Figure 4). As neuronal Plum is required for normal NMJ connectivity, we drove expression of the $Plum^{\Delta Cyt}$, $Plum^{\Delta Ig4}$, and $Plum^{\Delta Ig1\text{-}3}$ transgenes within the nervous system of $plum^{\Delta 2}$ larvae using the panneural elav-GAL4 driver. Similar to the MB, we observed a rescue of the mutant phenotype with the $Plum^{\Delta Cyt}$ and $Plum^{\Delta Ig1\text{-}3}$ transgenes, but not with the $Plum^{\Delta Ig4}$ transgene (Figure 7C). Thus, at the NMJ as in the MB, the C terminus of Plum is dispensable for its function, while the extracellular domain is essential.

Both the type I TGF-β receptor Babo and the ecdysone receptor EcR-B1 function at the NMJ in regulating synaptic growth (Ellis et al., 2010) and in the dismantling of synapses during metamorphosis (Liu et al., 2010), respectively. However, ensuring normal neuromuscular connectivity by preventing ectopic connections may be a qualitatively different process. Given the similarities of Plum action in MB γ axon pruning and in ensuring normal motoneuron connectivity in larvae, we tested whether Myo, Babo, and EcR-B1 play a role in the latter process. We found that RNAi knockdown of Myoglianin in muscle, but not in neurons, resulted in a significant increase of ectopic projection frequency, to the same extent as in the *plum* mutant (Figure 7C). $babo^{32/52}$ mutants also exhibited quantitatively similar phenotypes, as did larvae expressing a dominant-negative EcR transgene (Cherbas et al., 2003) driven by OK6-GAL4 in motoneurons (Figure 7C). Thus, both the TGF-β and ecdysone signaling pathways regulate larval neuromuscular connectivity.

To determine whether these effects were related to Plum, we examined ectopic projections in $plum^{\Delta 1/\Delta 2}$ larvae overexpressing EcR-B1 in all neurons. This manipulation significantly rescued the ectopic projection phenotype of *plum* mutants but did not itself have an ectopic phenotype (Figure 7C). In summary, as in the MB, Plum plays a role in developmental synaptic remodeling at the NMJ via EcR-B1, likely in response to muscle-derived TGF-β (Myo) signaling through the Baboon

receptor. In all, we conclude that Plum is not only required for MB neuronal remodeling but is also essential for normal neuromuscular connectivity, likely via the refinement of off-target ectopic connections of peripheral motoneuron terminals.

DISCUSSION

Using a forward genetic screen, we identified Plum, an IgSF transmembrane protein, as a key player in promoting the elimination of axonal and dendritic processes in mushroom body (MB) neurons. Plum acts cell autonomously in postmitotic neurons to promote axon pruning by regulating the expression of steroid hormone ecdysone receptor EcR-B1. Genetic and cell biological analyses indicate that Plum regulates EcR-B1 expression by facilitating TGF-β signaling, acting upstream of the type I receptor Baboon (Figure 6I). Remarkably, we found that the same pathway also functions in synapse refinement at the larval NMJ, highlighting its broad usage and conservation.

Possible Models by which Plum Facilitates TGF-β Signaling in MB Axon Pruning

Cell-cell interactions play an important role during neuronal remodeling to specify the temporal, and possibly spatial, extent of pruning (Bagri et al., 2003; Nikolaev et al., 2009; Zheng et al., 2003). Previous studies have identified the TGF-β type I receptor Babo and either of the type II receptors Wit or Punt as required for the initiation of MB γ axon pruning by regulating the expression of steroid hormone receptor EcR-B1 (Zheng et al., 2003). The strong genetic interactions between Plum, Babo, and Myo raised several possible models for Plum to participate in TGF-β signaling.

Plum could affect Babo cell-surface expression by, for example, functioning as a chaperone. This is consistent with our genetic epistasis experiments in which we could rescue the *plum* mutant phenotype by overexpressing Baboon in MB neurons. However, this model does not fit well with our finding that ectopic expression of $Plum^{\Delta Cyt}$ in glia affects pruning in MB neurons (Figure 6G). Moreover, glial or panneural ectopic overexpression of a secreted version of Plum's entire extracellular domain ($Plum^{ECD}$) similarly caused axon pruning defects in neighboring MB neurons (data not shown). These data argue against upregulation of Babo cell-surface expression as the primary mechanism of Plum action.

Plum could also act in a signaling pathway parallel to the canonical type I and II TGF-β receptors, Babo and Wit/Punt. In this model, the sum of signaling from both pathways could determine the expression levels of EcR-B1 and thus the pruning status. However, this model is not consistent with experiments in which pruning was inhibited by ectopically overexpressing $Plum^{\Delta Cyt}$ or $Plum^{ECD}$ in glial cells, unless the assumed Plum-dependent and Baboon-independent pathway is also activated by the TGF-β ligand Myo.

In another possible model, Plum functions by stabilizing the TGF-β receptor complex and/or facilitating TGF-β ligand binding, analogous to the roles played by accessory TGF-β receptors that have been described in mammals. Previous work in mammalian systems demonstrated that TGF-β type I/II receptor classic signaling is subject to modulation by accessory receptors, sometimes called type III receptors (Massagué, 1998). The TGF-β type III receptors Betaglycan and Endoglin are the most well-studied accessory receptors. Betaglycan is a membrane-anchored proteoglycan that facilitates binding of TGF-β2 to TβRII (Gatza et al., 2010). The role of TGF-β accessory receptors is not yet well understood, and they have been implicated in both facilitating, as well as inhibiting, TGF-β signaling (Shi and Massagué, 2003). A recent study has found that the Betaglycan extracellular ZP-C region adopts an immunoglobulin-like fold, despite sharing no sequence homology with Ig proteins, and possessing different disulfide linkages (Lin et al., 2011). The model by which Plum functions by stabilizing the TGF-β receptor complex and/or facilitating TGF-β ligand binding satisfactorily accounts for all the genetic interaction data, including the suppression of the *plum* phenotype by Baboon overexpression, as well as the pruning defect caused by glial misexpression of $Plum^{\Delta Cyt}$ or $Plum^{ECD}$. To test this hypothesis, we examined whether Plum physically interacts with the conventional type I/II receptors (Babo or Wit, respectively) or the TGF-β ligand (Myo). However, we have not been able to detect physical interactions of Plum with Myo, Babo, Wit, or their combinations under physiological conditions. Thus, although our genetic results suggest that Plum may act in an analogous fashion as the TGF-β accessory receptor described in previous mammalian studies, we could not support this model with conclusive biochemical data. Future studies are required to elucidate the exact mechanisms by which Plum relates to the canonical TGF-β receptors Babo, Wit/Punt, and the TGF-β ligand Myo.

Regardless of detailed mechanisms, our study has established a close connection between an IgSF protein and the TGF-β signaling pathway. Plum is a distant homolog of Protogenin and Nope, members of the DCC family that have been implicated in developmental processes, but their precise role is far from being understood (Salbaum and Kappen, 2000; Wong et al., 2010). Because of the broad roles of the TGF-β pathway in development and disease, it will be of great interest to determine whether other IgSF proteins act by facilitating TGF-β signaling.

Non-MB Plum May Regulate the Availability of the TGF-β Ligand Myoglianin

The availability and accessibility of TGF-β superfamily ligands fall under intricate regulation during animal development, with gastrulation being a hallmark example (De Robertis, 2009). Our results suggest that Plum might function within this network of regulation, in the context of MB axon pruning.

Axon pruning of MB γ neurons can be strongly influenced by nearby neurons, which also express Plum. The requirement for Plum within MB γ neurons during pruning is drastically reduced when neighboring neurons also lack Plum, compared to the situation in which all other cells are heterozygous for Plum (Figures 4J and 4L). Our Plum-Myo genetic interaction data (Figures 6G and 6H) suggest that Plum sequesters Myo, which can satisfactorily explain the above phenomenon. In a heterozygous background, Plum outside the γ-neuron clones sequesters Myo such that not enough ligand is available within the *plum* homozygous mutant clone to enable pruning. In a *plum* homozygous mutant animal, Myo is not sequestered. Therefore, higher

levels of Myo reach the MB and are sufficient to partly activate pruning. This sequestration model is further supported by our finding that overexpression of Plum$^{\Delta Cyt}$ or Plum^{ECD} (data not shown) by glia inhibits pruning in a dose-dependent manner and that concurrent glial overexpression of Myo suppresses the defect.

Plum as a General Regulator of Axon Remodeling during Development

Our identification of Plum as a cell-surface regulator of axon pruning has enriched our understanding of the mechanism by which extracellular signals trigger axon pruning. In addition to a role in MB γ neuron axon pruning, we also show that *plum* is involved in ensuring normal larval neuromuscular connectivity prior to metamorphosis. During motoneuron outgrowth in the embryo, both proper and off-target neuromuscular connections are formed. Off-target ectopic projections initially form as filopodial contacts (Jarecki and Keshishian, 1995) but are quickly removed. Delayed innervation (Kopczynski et al., 1996), impaired electrical activity (Jarecki and Keshishian, 1995), or chemorepulsion (Carrillo et al., 2010) cause a higher frequency of ectopic projections. Such connections are indistinguishable at the filopodial stage from normal growth cones (Halpern et al., 1991; Johansen et al., 1989; Murray et al., 1998) but persist and stabilize into ectopic connections. Several lines of evidence suggest that they are the result of reduced motoneuron pruning rather than improper sprouting (Carrillo et al., 2010). When normal innervation is delayed, the frequency of ectopic projections is increased (Kopczynski et al., 1996). However, after the muscle is finally innervated by its normal motoneuron, these connections are withdrawn. Similarly, increased ectopic connections due to reduced electrical activity are readily withdrawn following the restoration of activity during a critical period (Jarecki and Keshishian, 1995). Moreover, the requirement for chemorepulsion in preventing ectopic connections (Carrillo et al., 2010) suggests an active process of exclusion, inconsistent with improper sprouting. We found that in the *plum* mutant, increased ectopic connectivity is not accompanied by changes in bouton or branch number at normal NMJs (Figure S7). Taken together, these data suggest that normal connectivity at the NMJ and the prevention of off-target ectopic contacts arises through a process of synaptic refinement involving some form of motoneuron pruning, though not precisely analogous to the MB.

Our identification of *plum* suggests that the mechanism of larval neuromuscular refinement shares common molecular mechanisms with developmental MB axon pruning. Genetic studies suggest that, as in the MB, Plum functions to facilitate a TGF-β signal from the muscle upstream of EcR-B1 activity. Structure-function analysis identified the same domain requirement of Plum in promoting the refinement of ectopic motor axons as MB γ neuron pruning. Cell-type-specific rescue experiments are consistent with neuronal Plum interacting via a heterophilic partner. This heterophilic partner may indeed be Myoglianin, as muscle knockdown of Myo phenocopies the *plum* mutant. Such a mechanism is consistent with the involvement of other muscle-derived ligands in preventing ectopic connection formation (Winberg et al., 1998). At the NMJ, Plum regulates one aspect of synaptic refinement, conveying a signal that can cooperate with others to maintain normal connectivity. Our findings mechanistically connect two disparate processes of developmental axon remodeling and highlight the general involvement of the Plum-Babo-Myo-EcR pathway in neuronal process refinement during development.

EXPERIMENTAL PROCEDURES

MARCM-Based Forward Genetic Screen

We used ethyl methane sulfonate (EMS; 25 mM in sucrose solution) to mutagenize male flies carrying FRT2A and FRT82B, which are sites for the FLP-mediated recombination on the left and right arms of the third chromosome, respectively. After establishing individual mutant stocks and confirming the lethality of mutations located on FRT-containing third chromosomes, we crossed these mutants to a "MARCM-ready fly stock" (for the third chromosome right arm screen: *y*, *w*, *hsFlp122*, UAS-*m*CD8-*GFP;* 201Y-GAL4, UAS-*m*CD8-*GFP* / *CyO; FRT82B*, *tubP*-Gal80 / *TM6*, *Tb*). Cross progeny were heat shocked for 40–60 min at 37°C at 20–28 hr after egg laying. We then dissected out the adult fly brains of the appropriate genotype as previously described (Wu and Luo, 2006) and analyzed MB γ neurons by visualizing expression of mCD8-GFP in whole-mount live or fixed brains using a compound fluorescent microscope.

An intrinsic feature of mosaic analysis with MARCM is that once a clone is generated, no new functional mRNA or protein is made in mutant cells. Nevertheless, pre-existing mRNAs and proteins inherited from heterozygous parental cells can persist and function normally for a certain period of time, resulting in perdurance. Therefore, the amount of protein perdurance depends on the number of divisions the parental cell undergoes before the postmitotic cell is born. Because single cell clones are generated from a single cell division of the ganglion mother cell (in which the mitotic recombination occurs), the mRNA and proteins are diluted by only a factor of two. In contrast, neuroblast clones include neurons that are at least two cell divisions from the neuroblast in which the recombination occurred. Thus, protein perdurance could strongly affect single cell clones.

Generation and Imaging MARCM Clones

MB MARCM neuroblast or single cell clones were generated by heat shocking newly hatched larvae and examined as described previously (Lee et al., 1999). Brains were mounted in Slowfade (Invitrogen, Carlsbad, CA, USA), whereas larvae (for NMJ analysis) were mounted in Vectashield (Vector Laboratories, Burlingame, CA, USA) and imaged on Zeiss LSM510 or LSM710 confocal microscopes.

Genetic Mapping of *plum*

Genetic mapping for the causal gene in EMS$^{4\text{-}39}$ was performed by first using SNP-based recombination mapping (Berger et al., 2001). This mapping narrowed the suspected region to a cytological location between 97A10 and 97C5 and at the same time eliminated the lethal mutation(s) on the third chromosome, revealing that EMS$^{4\text{-}39}$ was actually not homozygous lethal. At this point, because of a lack of more informative SNPs within the suspected region, we continued the mapping by generating molecularly defined chromosomal deletions and testing the phenotypes of EMS$^{4\text{-}39}$/deletions compound heterozygous flies. We used FLP-mediated *trans*-recombination to generate deletions as previously described (Parks et al., 2004). The two informative deletions, as well as the flies used to generate them, are depicted in Figure S1.

Cloning *plum*

At the time we cloned *plum*, the annotated *CG6490* sequence was incomplete and did not contain a signal peptide. We therefore performed 5′ rapid amplification of cDNA ends (RACE) using the Invitrogen GeneRacer Kit. We obtained the full-length RNA of *plum* and uncovered two additional upstream exons, encoding a protein that contained a signal peptide. The full-length *plum* sequence is available in GenBank, under accession number JF268497.

Neuromuscular Ectopic Projection Analysis

Wandering third-instar larvae were dissected and processed as previously described (Mosca and Schwarz, 2010). During imaging, the HRP channel was artificially enhanced to reveal low-level background staining of the underlying muscles. Two kinds of ectopic projections were scored: improper connections from the transverse nerve, which runs along the segment border, onto muscles 6 or 7 or improper connections onto muscle 6 from the other motoneurons that normally avoid this muscle. Phenotypes were calculated as the number of body wall hemisegments containing one or more ectopic connections. Statistical significance was calculated using an ANOVA with a Dunnett post hoc comparison to the control sample. Error bars represent ± SEM. ***, $p < 0.001$.

Immunofluorescence Antibody Conditions

The following antibody conditions were used: rat monoclonal anti-mouse CD8 α subunit, 1:100 (Caltag, Burlingame, CA, USA); rabbit polyclonal anti-HA (ab9110), 1:2,000 (Abcam, Cambridge, MA, USA); mouse monoclonal anti-HA (12CA5), 1:100 (Abcam); mouse monoclonal anti-Flag M2 antibody (F1804), 1:100 (Sigma-Aldrich, St. Louis); mouse α-Brp, 1:250 (Wagh et al., 2006); rabbit α-Synaptotagmin I, 1:4,000 (Mackler et al., 2002); mouse monoclonal anti-FasII (1D4), 1:50 (Developmental Studies Hybridoma Bank, University of Iowa, Iowa City, IA, USA). Alexa488, Alexa546, or Alexa633-conjugated secondary antibodies were used at 1:300 (Invitrogen). FITC-conjugated antibodies to horseradish peroxidase (HRP) were used at 1:100 to visualize nerves (Jackson ImmunoResearch, West Grove, PA, USA). For staining of plumBAC-GFP:HA, samples were first incubated with mouse anti-HA (12CA5), then H_2O_2 treated for 10 min, incubated with Biotin-conjugated goat anti-mouse (Jackson ImmunoResearch), signal amplified with an ABC-Amplification Kit (Vector Labs), and incubated with Cy5-tyramide (1:400) for 5 min.

Characterization of Pruning Defect Severity and Fly Survival

The severity of γ MARCM clone pruning defects in the adult brain is categorized based on whether the clone innervates the adult γ lobe and whether it contains dorsal unpruned axonal branches. The adult γ lobe is defined by moderate FasII immunoreactivity, usually labeled with an asterisk in figures. Dorsal unpruned axonal branches are those that are significantly outside the α lobe, which is defined by strong FasII immunoreactivity.

For Figure 6H, γ neurons were visualized by FasII antibody staining. The different categories of pruning defect severity are defined as such: strong, no γ neurons innervate the adult γ lobe; medium, innervation of the adult γ lobe is seen but the majority of γ neurons are unpruned; and mild, the adult γ lobe is substantially innervated, and unpruned γ neurons are sparse. For Figure 6I, the survival rate was calculated as the number of flies surviving to adulthood divided by the genetically expected number of flies of a given genotype.

ACCESSION NUMBERS

The GenBank accession number for the full-length *plum* sequence reported in this paper is JF268497.

SUPPLEMENTAL INFORMATION

Supplemental Information includes seven figures and Supplemental Experimental Procedures and can be found with this article online at http://dx.doi.org/10.1016/j.neuron.2013.03.004.

ACKNOWLEDGMENTS

We thank L. Attisano, T. Lee, M. B. O'Connor, N. Reist, the Vienna *Drosophila* RNAi Center, and the Bloomington stock center for reagents; the FasII (1D4) and Brp (nc82) monoclonal antibodies were obtained from the Developmental Studies Hybridoma Bank developed under the auspices of the National Institute of Child Health and Human Development and maintained by the University of Iowa. We also thank R. Watts and E. Hoopfer for many hours of joint screening, N. Goriatcheva, D. Luginbuhl, N. Issman, and O. Fuchs for technical assistance, O. Golani for help with MATLAB programming, M. Hortsch and M. Serpe for discussions, and K. Shen, A. Yaron, M. Schuldiner, and members of the Luo and Schuldiner labs for discussions and their critical reading of our manuscript. This work was supported by a grant from the National Institutes of Health (NIH) (R37-NS041044) (to L.L.), by grants from the Israel Science Foundation (1864/08 and 683/11) (Bio-med Legacy program), funds from the Irving B. Harrison foundation, the Estate of Florence and Charles Cuevas, and the Adelis Foundation (to O.S.). L.L. and K.C.G. are investigators of the Howard Hughes Medical Institute. O.S. is the incumbent of the Rothstein Career Development Chair of Genetic Diseases. T.J.M. was supported by Epilepsy, Neonatology, and Developmental Biology Training grants (NIH) (5T32 NS 007280 and HD007249). X.M.Y. was a Damon Runyon Fellow supported by the Damon Runyon Cancer Research Foundation (DRG1993-08).

Accepted: February 26, 2013
Published: May 8, 2013

REFERENCES

Agarwala, K.L., Nakamura, S., Tsutsumi, Y., and Yamakawa, K. (2000). Down syndrome cell adhesion molecule DSCAM mediates homophilic intercellular adhesion. Brain Res. Mol. Brain Res. *79*, 118–126.

Awasaki, T., and Ito, K. (2004). Engulfing action of glial cells is required for programmed axon pruning during Drosophila metamorphosis. Curr. Biol. *14*, 668–677.

Awasaki, T., Tatsumi, R., Takahashi, K., Arai, K., Nakanishi, Y., Ueda, R., and Ito, K. (2006). Essential role of the apoptotic cell engulfment genes draper and ced-6 in programmed axon pruning during Drosophila metamorphosis. Neuron *50*, 855–867.

Awasaki, T., Huang, Y., O'Connor, M.B., and Lee, T. (2011). Glia instruct developmental neuronal remodeling through TGF-β signaling. Nat. Neurosci. *14*, 821–823.

Bagri, A., Cheng, H.J., Yaron, A., Pleasure, S.J., and Tessier-Lavigne, M. (2003). Stereotyped pruning of long hippocampal axon branches triggered by retraction inducers of the semaphorin family. Cell *113*, 285–299.

Berger, J., Suzuki, T., Senti, K.A., Stubbs, J., Schaffner, G., and Dickson, B.J. (2001). Genetic mapping with SNP markers in Drosophila. Nat. Genet. *29*, 475–481.

Bishop, D.L., Misgeld, T., Walsh, M.K., Gan, W.B., and Lichtman, J.W. (2004). Axon branch removal at developing synapses by axosome shedding. Neuron *44*, 651–661.

Boulanger, A., Clouet-Redt, C., Farge, M., Flandre, A., Guignard, T., Fernando, C., Juge, F., and Dura, J.M. (2011). ftz-f1 and Hr39 opposing roles on EcR expression during Drosophila mushroom body neuron remodeling. Nat. Neurosci. *14*, 37–44.

Brummel, T., Abdollah, S., Haerry, T.E., Shimell, M.J., Merriam, J., Raftery, L., Wrana, J.L., and O'Connor, M.B. (1999). The Drosophila activin receptor baboon signals through dSmad2 and controls cell proliferation but not patterning during larval development. Genes Dev. *13*, 98–111.

Brümmendorf, T., and Rathjen, F.G. (1996). Structure/function relationships of axon-associated adhesion receptors of the immunoglobulin superfamily. Curr. Opin. Neurobiol. *6*, 584–593.

Carrillo, R.A., Olsen, D.P., Yoon, K.S., and Keshishian, H. (2010). Presynaptic activity and CaMKII modulate retrograde semaphorin signaling and synaptic refinement. Neuron *68*, 32–44.

Cherbas, L., Hu, X., Zhimulev, I., Belyaeva, E., and Cherbas, P. (2003). EcR isoforms in Drosophila: testing tissue-specific requirements by targeted blockade and rescue. Development *130*, 271–284.

De Robertis, E.M. (2009). Spemann's organizer and the self-regulation of embryonic fields. Mech. Dev. *126*, 925–941.

Eaton, B.A., Fetter, R.D., and Davis, G.W. (2002). Dynactin is necessary for synapse stabilization. Neuron *34*, 729–741.

Ellis, J.E., Parker, L., Cho, J., and Arora, K. (2010). Activin signaling functions upstream of Gbb to regulate synaptic growth at the Drosophila neuromuscular junction. Dev. Biol. *342*, 121–133.

Gatza, C.E., Oh, S.Y., and Blobe, G.C. (2010). Roles for the type III TGF-beta receptor in human cancer. Cell. Signal. *22*, 1163–1174.

Gesualdi, S.C., and Haerry, T.E. (2007). Distinct signaling of Drosophila Activin/TGF-beta family members. Fly (Austin) *1*, 212–221.

Halpern, M.E., Chiba, A., Johansen, J., and Keshishian, H. (1991). Growth cone behavior underlying the development of stereotypic synaptic connections in Drosophila embryos. J. Neurosci. *11*, 3227–3238.

Hoopfer, E.D., McLaughlin, T., Watts, R.J., Schuldiner, O., O'Leary, D.D., and Luo, L. (2006). Wlds protection distinguishes axon degeneration following injury from naturally occurring developmental pruning. Neuron *50*, 883–895.

Islam, R., Kristiansen, L.V., Romani, S., Garcia-Alonso, L., and Hortsch, M. (2004). Activation of EGF receptor kinase by L1-mediated homophilic cell interactions. Mol. Biol. Cell *15*, 2003–2012.

Ito, K., Awano, W., Suzuki, K., Hiromi, Y., and Yamamoto, D. (1997). The Drosophila mushroom body is a quadruple structure of clonal units each of which contains a virtually identical set of neurones and glial cells. Development *124*, 761–771.

Jarecki, J., and Keshishian, H. (1995). Role of neural activity during synaptogenesis in Drosophila. J. Neurosci. *15*, 8177–8190.

Johansen, J., Halpern, M.E., and Keshishian, H. (1989). Axonal guidance and the development of muscle fiber-specific innervation in Drosophila embryos. J. Neurosci. *9*, 4318–4332.

Kantor, D.B., and Kolodkin, A.L. (2003). Curbing the excesses of youth: molecular insights into axonal pruning. Neuron *38*, 849–852.

Kopczynski, C.C., Davis, G.W., and Goodman, C.S. (1996). A neural tetraspanin, encoded by late bloomer, that facilitates synapse formation. Science *271*, 1867–1870.

Kuo, C.T., Zhu, S., Younger, S., Jan, L.Y., and Jan, Y.N. (2006). Identification of E2/E3 ubiquitinating enzymes and caspase activity regulating Drosophila sensory neuron dendrite pruning. Neuron *51*, 283–290.

Lee, T., and Luo, L. (1999). Mosaic analysis with a repressible cell marker for studies of gene function in neuronal morphogenesis. Neuron *22*, 451–461.

Lee, T., Lee, A., and Luo, L. (1999). Development of the Drosophila mushroom bodies: sequential generation of three distinct types of neurons from a neuroblast. Development *126*, 4065–4076.

Lee, T., Marticke, S., Sung, C., Robinow, S., and Luo, L. (2000). Cell-autonomous requirement of the USP/EcR-B ecdysone receptor for mushroom body neuronal remodeling in Drosophila. Neuron *28*, 807–818.

Lin, S.J., Hu, Y., Zhu, J., Woodruff, T.K., and Jardetzky, T.S. (2011). Structure of betaglycan zona pellucida (ZP)-C domain provides insights into ZP-mediated protein polymerization and TGF-beta binding. Proc. Natl. Acad. Sci. USA *108*, 5232–5236.

Liu, X.B., Low, L.K., Jones, E.G., and Cheng, H.J. (2005). Stereotyped axon pruning via plexin signaling is associated with synaptic complex elimination in the hippocampus. J. Neurosci. *25*, 9124–9134.

Liu, Z., Chen, Y., Wang, D., Wang, S., and Zhang, Y.Q. (2010). Distinct presynaptic and postsynaptic dismantling processes of Drosophila neuromuscular junctions during metamorphosis. J. Neurosci. *30*, 11624–11634.

Luo, L., and O'Leary, D.D. (2005). Axon retraction and degeneration in development and disease. Annu. Rev. Neurosci. *28*, 127–156.

Mackler, J.M., Drummond, J.A., Loewen, C.A., Robinson, I.M., and Reist, N.E. (2002). The C(2)B Ca(2+)-binding motif of synaptotagmin is required for synaptic transmission in vivo. Nature *418*, 340–344.

Massagué, J. (1998). TGF-beta signal transduction. Annu. Rev. Biochem. *67*, 753–791.

Massaro, C.M., Pielage, J., and Davis, G.W. (2009). Molecular mechanisms that enhance synapse stability despite persistent disruption of the spectrin/ankyrin/microtubule cytoskeleton. J. Cell Biol. *187*, 101–117.

Mosca, T.J., and Schwarz, T.L. (2010). The nuclear import of Frizzled2-C by Importins-beta11 and alpha2 promotes postsynaptic development. Nat. Neurosci. *13*, 935–943.

Murray, M.J., Merritt, D.J., Brand, A.H., and Whitington, P.M. (1998). In vivo dynamics of axon pathfinding in the Drosophilia CNS: a time-lapse study of an identified motorneuron. J. Neurobiol. *37*, 607–621.

Nguyen, Q.T., and Lichtman, J.W. (1996). Mechanism of synapse disassembly at the developing neuromuscular junction. Curr. Opin. Neurobiol. *6*, 104–112.

Nikolaev, A., McLaughlin, T., O'Leary, D.D., and Tessier-Lavigne, M. (2009). APP binds DR6 to trigger axon pruning and neuron death via distinct caspases. Nature *457*, 981–989.

Parks, A.L., Cook, K.R., Belvin, M., Dompe, N.A., Fawcett, R., Huppert, K., Tan, L.R., Winter, C.G., Bogart, K.P., Deal, J.E., et al. (2004). Systematic generation of high-resolution deletion coverage of the Drosophila melanogaster genome. Nat. Genet. *36*, 288–292.

Pielage, J., Fetter, R.D., and Davis, G.W. (2005). Presynaptic spectrin is essential for synapse stabilization. Curr. Biol. *15*, 918–928.

Portera-Cailliau, C., Weimer, R.M., De Paola, V., Caroni, P., and Svoboda, K. (2005). Diverse modes of axon elaboration in the developing neocortex. PLoS Biol. *3*, e272.

Raff, M.C., Whitmore, A.V., and Finn, J.T. (2002). Axonal self-destruction and neurodegeneration. Science *296*, 868–871.

Rougon, G., and Hobert, O. (2003). New insights into the diversity and function of neuronal immunoglobulin superfamily molecules. Annu. Rev. Neurosci. *26*, 207–238.

Salbaum, J.M., and Kappen, C. (2000). Cloning and expression of nope, a new mouse gene of the immunoglobulin superfamily related to guidance receptors. Genomics *64*, 15–23.

Schuldiner, O., Berdnik, D., Levy, J.M., Wu, J.S., Luginbuhl, D., Gontang, A.C., and Luo, L. (2008). piggyBac-based mosaic screen identifies a postmitotic function for cohesin in regulating developmental axon pruning. Dev. Cell *14*, 227–238.

Schuster, C.M., Davis, G.W., Fetter, R.D., and Goodman, C.S. (1996). Genetic dissection of structural and functional components of synaptic plasticity. I. Fasciclin II controls synaptic stabilization and growth. Neuron *17*, 641–654.

Shi, Y., and Massagué, J. (2003). Mechanisms of TGF-beta signaling from cell membrane to the nucleus. Cell *113*, 685–700.

Truman, J.W. (1990). Metamorphosis of the central nervous system of Drosophila. J. Neurobiol. *21*, 1072–1084.

Vogel, C., Teichmann, S.A., and Chothia, C. (2003). The immunoglobulin superfamily in Drosophila melanogaster and Caenorhabditis elegans and the evolution of complexity. Development *130*, 6317–6328.

Wagh, D.A., Rasse, T.M., Asan, E., Hofbauer, A., Schwenkert, I., Dürrbeck, H., Buchner, S., Dabauvalle, M.C., Schmidt, M., Qin, G., et al. (2006). Bruchpilot, a protein with homology to ELKS/CAST, is required for structural integrity and function of synaptic active zones in Drosophila. Neuron *49*, 833–844.

Watts, R.J., Hoopfer, E.D., and Luo, L. (2003). Axon pruning during Drosophila metamorphosis: evidence for local degeneration and requirement of the ubiquitin-proteasome system. Neuron *38*, 871–885.

Watts, R.J., Schuldiner, O., Perrino, J., Larsen, C., and Luo, L. (2004). Glia engulf degenerating axons during developmental axon pruning. Curr. Biol. *14*, 678–684.

Williams, D.W., Kondo, S., Krzyzanowska, A., Hiromi, Y., and Truman, J.W. (2006). Local caspase activity directs engulfment of dendrites during pruning. Nat. Neurosci. *9*, 1234–1236.

Winberg, M.L., Mitchell, K.J., and Goodman, C.S. (1998). Genetic analysis of the mechanisms controlling target selection: complementary and combinatorial functions of netrins, semaphorins, and IgCAMs. Cell *93*, 581–591.

Wong, Y.H., Lu, A.C., Wang, Y.C., Cheng, H.C., Chang, C., Chen, P.H., Yu, J.Y., and Fann, M.J. (2010). Protogenin defines a transition stage during embryonic neurogenesis and prevents precocious neuronal differentiation. J. Neurosci. *30*, 4428–4439.

Wu, J.S., and Luo, L. (2006). A protocol for dissecting Drosophila melanogaster brains for live imaging or immunostaining. Nat. Protoc. *1*, 2110–2115.

Yang, M.Y., Armstrong, J.D., Vilinsky, I., Strausfeld, N.J., and Kaiser, K. (1995). Subdivision of the Drosophila mushroom bodies by enhancer-trap expression patterns. Neuron *15*, 45–54.

Zheng, X., Wang, J., Haerry, T.E., Wu, A.Y., Martin, J., O'Connor, M.B., Lee, C.H., and Lee, T. (2003). TGF-beta signaling activates steroid hormone receptor expression during neuronal remodeling in the Drosophila brain. Cell *112*, 303–315.

Neuron, Volume *78*

Supplemental Information

Plum, an Immunoglobulin Superfamily Protein, Regulates Axon Pruning by Facilitating TGF-β Signaling

Xiaomeng M. Yu, Itai Gutman, Timothy J. Mosca, Tal Iram, Engin Özkan, K. Christopher Garcia, Liqun Luo, and Oren Schuldiner

Inventory of Supplemental Information

Supplemental Figures

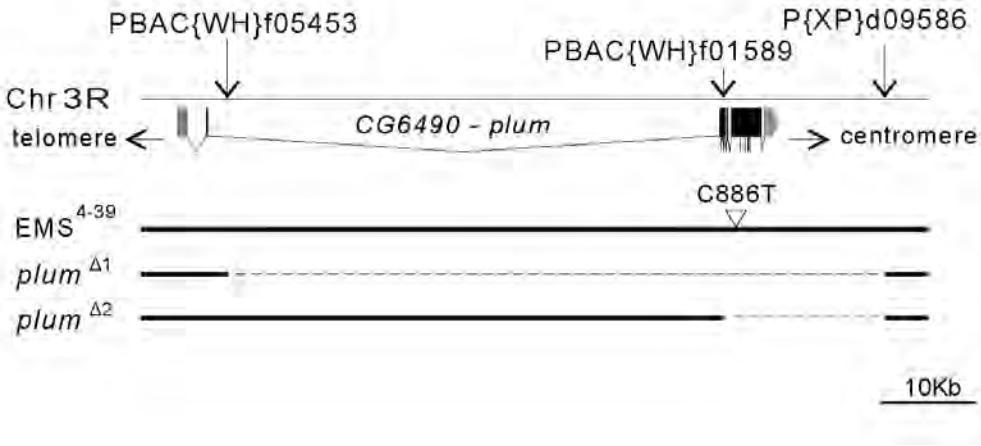

Figure S1. Genomic Structure of the *plum* Gene and Alleles, Relates to Figure 1.
plum genomic structure depicting the location of the EMS$^{4-39}$ mutation and the *plum*$^{\Delta 1}$ and *plum*$^{\Delta 2}$ deletions. Dashed lines indicate deleted genomic sequences. P[XP]d09586, pBAC[WH]f01589 and pBAC[WH]f05453 are FRT containing transposons used to generate the *plum*$^{\Delta 1}$ and *plum*$^{\Delta 2}$ deletions. Gray bars, UTRs; black bars, coding regions.

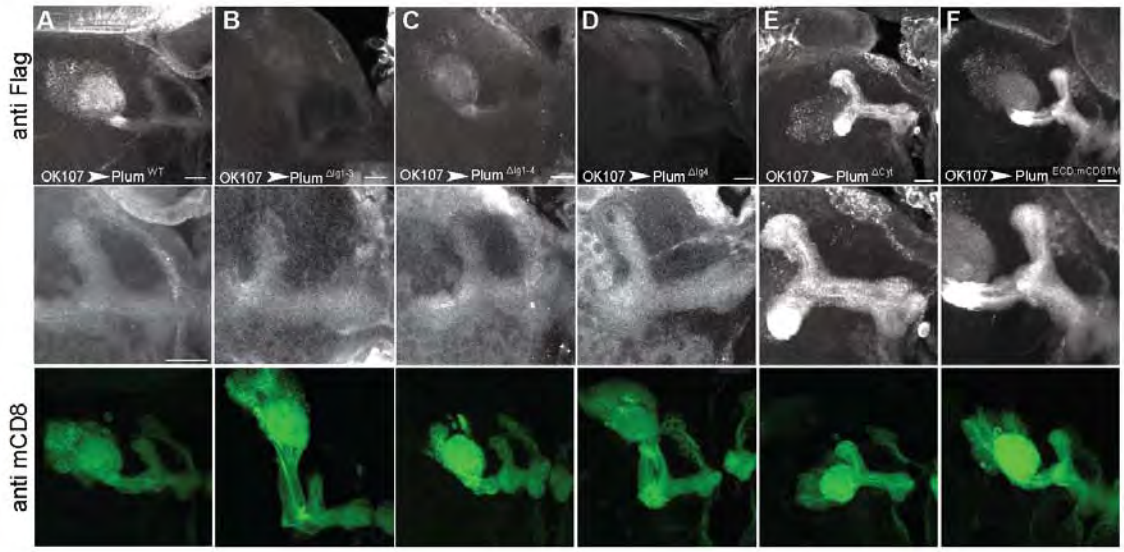

Figure S2. Expression of Transgenes Used in Structure-Function Analysis, Relates to Figure 3.

(A-F) Confocal Z-projections of OK107-GAL4 driven Plum^{transgene}:Flag in late larval brains. Upper panels are anti-Flag staining showing the expression levels and subcellular distributions of Plum transgenes. Images were taken with identical laser and gain parameters on the confocal and were not modified in the upper panels for better comparison. Middle panels are Z-stack projections of subsets of the same images, from the axon lobe regions, in which we modified the contrast and brightness for optimized visualization. Lower panels are mCD8::GFP expression. Note that despite lower transgene expression in B, C and D, there is no correlation between expression and rescue ability – for example, expression is similarly low in (B) Plum$^{\Delta Ig1-3}$ and (D) Plum$^{\Delta Ig4}$ transgenes but only the former rescues the pruning defects (see Figure 3). Scale bar, 20μm.

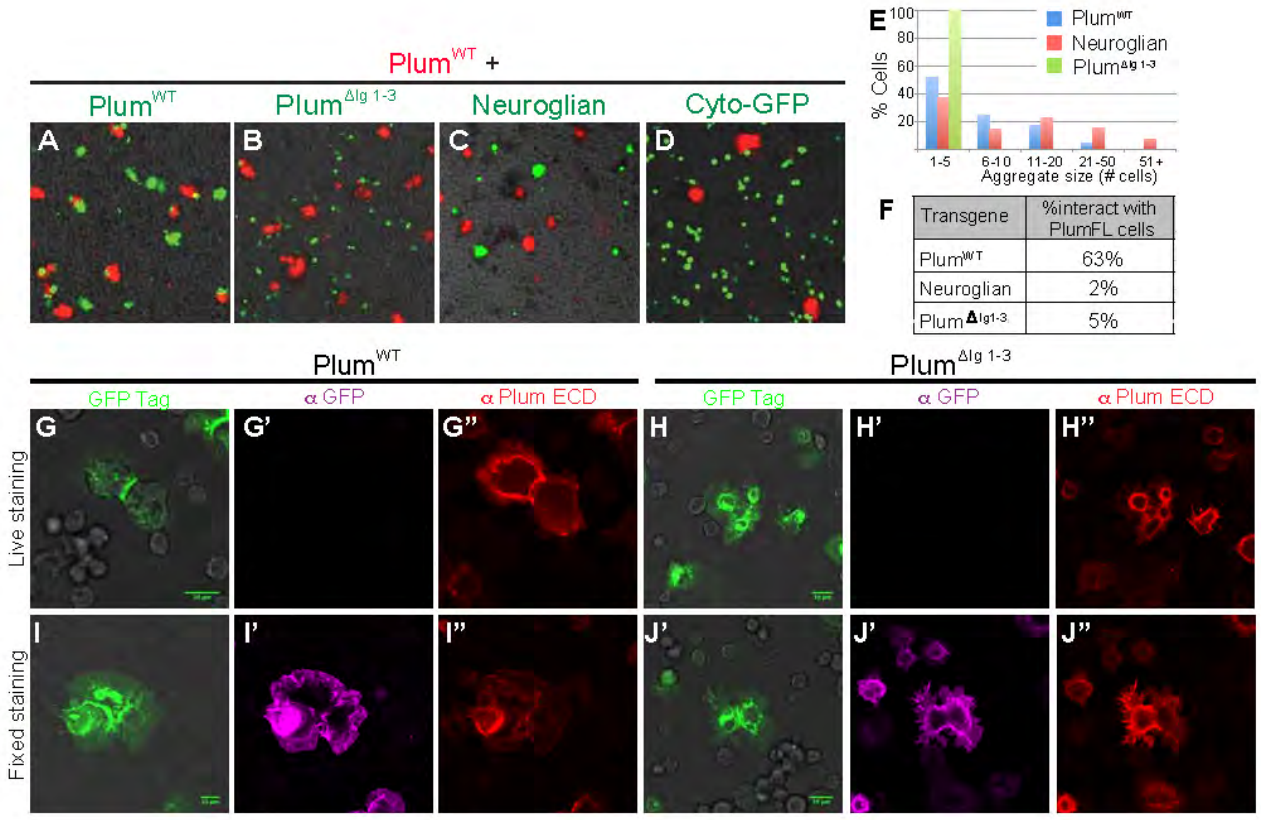

Figure S3. Plum Homophilic Interactions Are Not Required for Axon Pruning, Related to Figure 3.

(A-D) Representative images of aggregation assays resulting from the mixing of differently transfected S2 cells. Mixtures contained cells transfected with (A-D) Actin5C-*plum*^{WT}:mRFP and cells transfected with (A) Actin5C-*plum*^{WT}:GFP, (B) Actin5C-*plum*$^{\Delta Ig1-3}$*:GFP*, (C) Actin5C-*Neuroglian:GFP* or (D) Actin5C-*GFP*.

(E) Histogram distribution of homophilic (between GFP^{+} cells only) aggregation sizes of differently transfected S2 cells (see Supplemental Experimental Procedures).

(F) Percentage of GFP^{+} aggregates (aggregate size >5 cells) that also form aggregates with *plum*^{WT}:mRFP expressing cells (see Supplemental Experimental Procedures).

(G-J) Plum^{WT} and Plum$^{\Delta Ig1-3}$ are both expressed on the membrane surface. (G, I) Single confocal slices of S2 cells expressing Actin5C-*plum*^{WT}:GFP (Plum^{WT}) or (H, J) Actin5C-*plum*$^{\Delta Ig1-3}$*:GFP* (Plum$^{\Delta 1-3}$). Cells were either fixed (G, H) or not (I, J) before antibody staining. Left panels are GFP fluorescence; middle panels are anti-GFP staining; right panels are anti-Plum (see Supplemental Experimental Procedures).

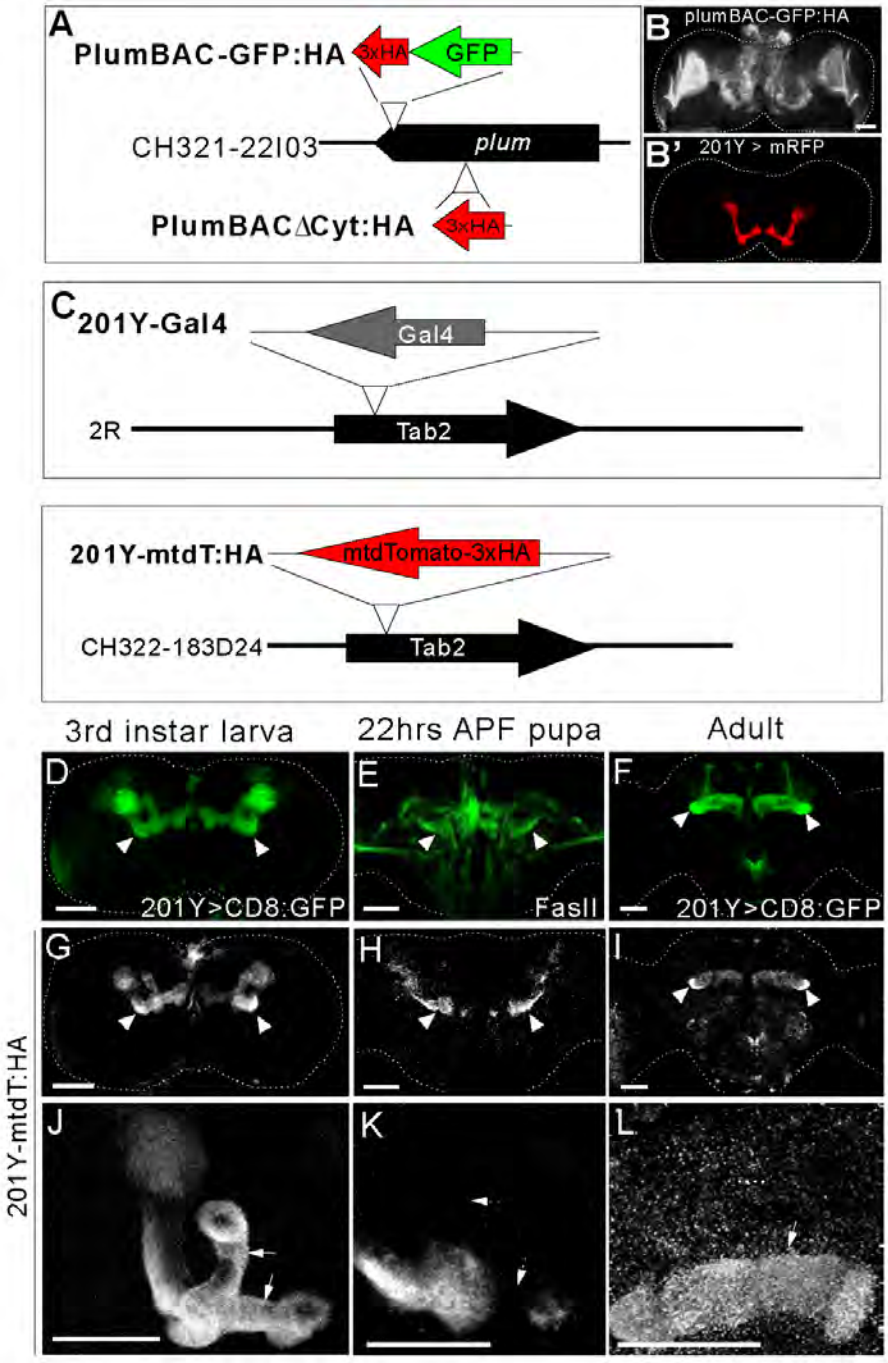

Figure S4. Recombineered BAC Transgenes, Relates to Figure 4.
(A) Both PlumBAC-GFP:HA and PlumBACΔCyt:HA were created from recombineering an insertion into the *plum*-containing BAC clone CH321-22I03 (91kb) using methods described previously (Venken et al, 2009). PlumBAC-GFP:HA inserts GFP-3xHA immediately after the last amino acid codon. plumBACΔCyt:HA inserts a 3xHA tag (with STOP codon) after residue 944 (Glycine), 9 amino acids C terminal to the predicted transmembrane domain, effectively creating a truncated version of the Plum expression transgene. Both transgenes were integrated at the attP-VK37 site (Venken et al., 2009) by BestGene.

(B) Confocal Z-projections of a WT brain expressing plumBAC-GFP:HA. Upper panel is anti-Plum staining while lower panel is 201Y-GAL4 driven myr-RFP. Scale bar is 20 μm.
(C) Upper panel: diagram of 201Y-GAL4 enhancer trap, where GAL4 is inserted into Tab2 gene in antisense direction. Immediate 3' flanking sequence of 201Y-GAL4: GACAAGGCTGTTAAATATTT. Lower panel: 201Y-mtdT:HA was created by inserting mtdTomato-3xHA into a Tab2-containing BAC clone (CH322-183D24) at exactly the same position as the 201Y-GAL4 enhancer trap and also in antisense orientation. The transgene was integrated at attP-VK2.
(D-L) Comparing expression pattern of 201Y-mtdT:HA with 201Y-GAL4 driving mCD8:GFP as well as FasII staining at different developmental stages. Arrowheads indicate mushroom body. Arrows indicate dorsal and medial γ lobes. Dashed arrows indicate pruned larval γ lobes. At late larval stage (D, G, J), 201Y-mtdT:HA appears identical to 201Y-GAL4 driving mCD8:GFP. At 22hrs APF (E, H, K), 201Y-mtdT:HA revealed γ axon degeneration (K). Unlike FasII staining at this stage (E), 201Y-mtdT:HA is specific for γ neurons (H, K). At adult stage (F, I, L), 201Y-mtdT:HA appear weaker than 201Y-GAL4 driving the expression of mCD8:GFP. It also does not label α/β lobe as significantly. Scale bar is 20 μm.

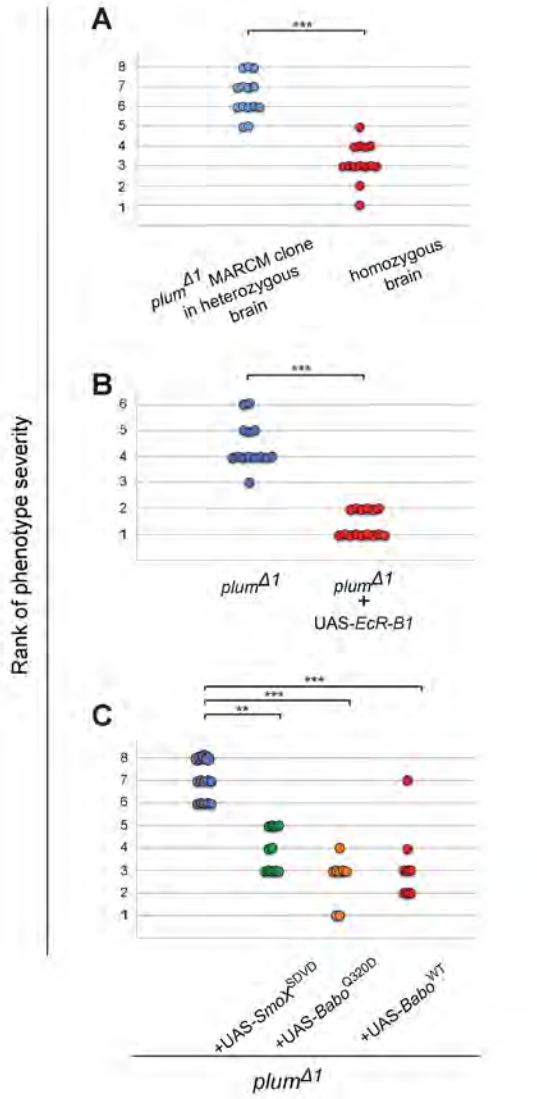

Figure S5. Rank Order Tests for Pruning Defects, Related to Figures 4-6.

(A) Quantification of the pruning defect severity of *plum*$^{\Delta 1}$ MB MARCM neuroblast clones within *plum*$^{\Delta 1}$ (red; n=15) or *plum*$^{\Delta 1/+}$ (blue; n=13) brains, related to Figure 4 J-K.

(B) Quantification of the pruning defect severity of *plum*$^{\Delta 1}$ MB MARCM neuroblast clones (blue; n=14) or *plum*$^{\Delta 1}$ additionally expressing UAS-EcR-B1 (red; n=15) brains, related to Figure 5E-F.

(C) Quantification of the pruning defect severity of *plum*$^{\Delta 1}$ MB MARCM neuroblast clones (blue; n=14) or *plum*$^{\Delta 1}$ additionally expressing UAS-Babo^{WT} (red; n=8), UAS-Babo^{Q320D} (orange; n=8) or UAS-SmoX^{SDVD} (green; n=11) brains, related to Figure 6B-F.

To analyze the severity of the pruning phenotypes, confocal Z-projections from the appropriate genotypes were rank ordered in a double-blind fashion based on the severity of their pruning defect. The severity was determined by comparing the unpruned dorsal γ-axons to pruned γ-axons in the adult-specific medial lobe; these pruned axons can be distinguished from unpruned medial axons, as they branch extensively and are located at a more dorsal and posterior position. ANOVA with a Kruskal-Wallis post-hoc test was used to determine significance: ***, $p < 0.001$; **, $p<0.01$.

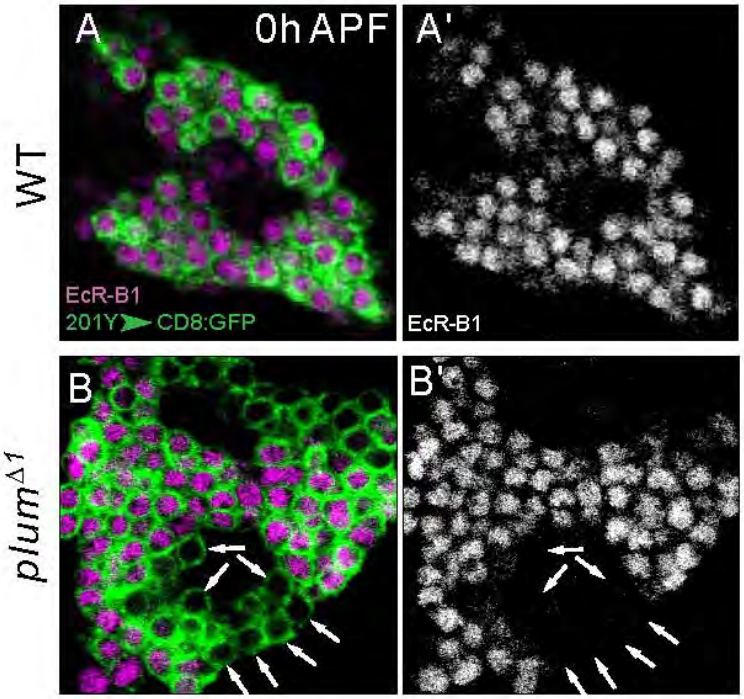

Figure S6. Partial loss of EcR-B1 expression in homozygous *plum*$^{\Delta 1}$ brains, Related to Figure 5.

Single confocal sections of 0 hr APF MB cell bodies in (A) WT (n=6), (B) *plum*$^{\Delta 1}$ homozygous brains (n=5). Green labels γ neurons. Magenta indicates EcR-B1 expression. Arrows in B point to cell bodies that do not express EcR-B1.

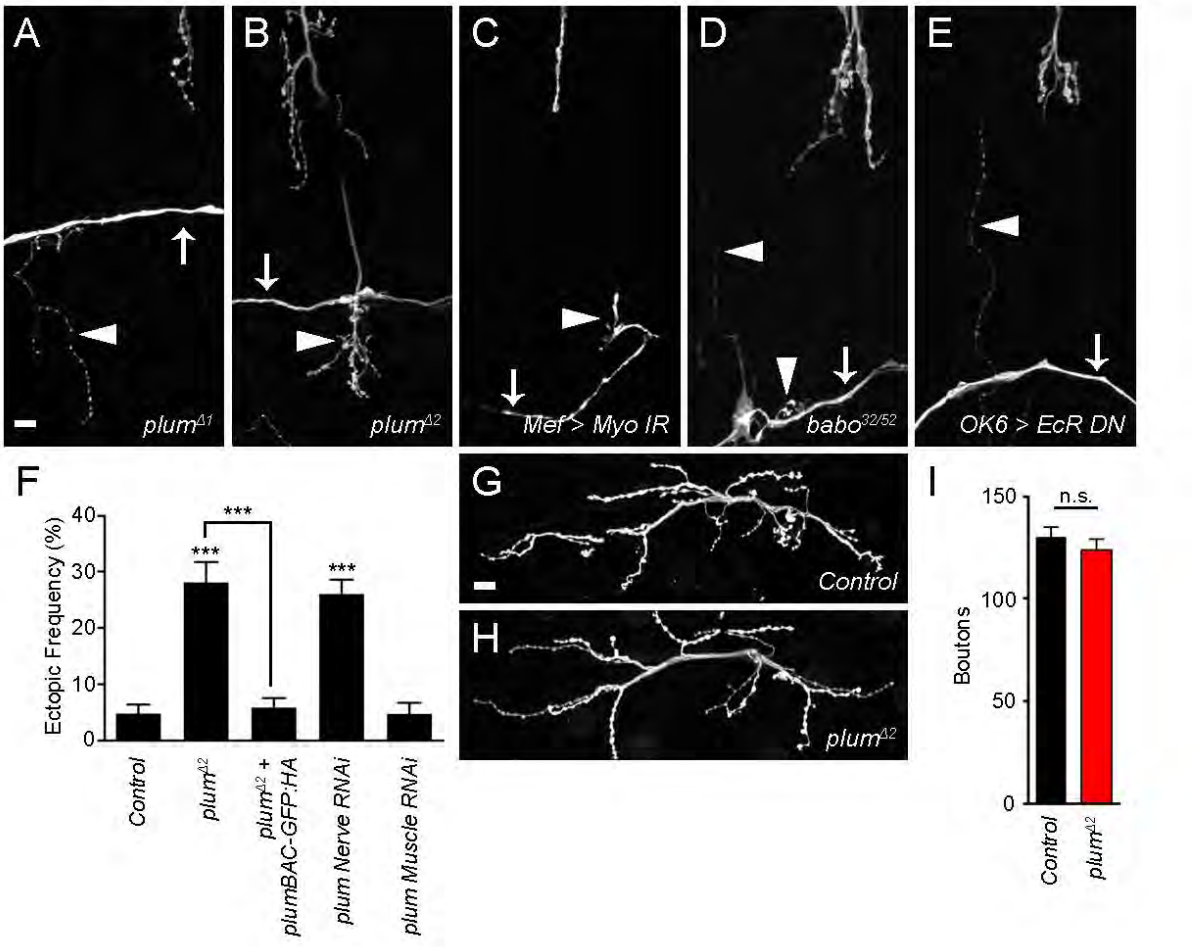

Figure S7. *plum* Phenotypes at the *Drosophila* Larval NMJ, Relates to Figure 7.
(A-D): (A) Additional examples of ectopic connections from the transverse nerve onto muscles 6 and 7 in $plum^{\Delta 1}$, (B) $plum^{\Delta 2}$, (C) Mef2-GAL4 > UAS-myo^{RNAi}, (D) $babo^{32/52}$, and (E) OK6-GAL4 > UAS-EcR-DN, larvae. In all cases, the transverse nerve (arrow) makes inappropriate connections (arrowhead) with the muscles that are otherwise normally innervated. In all panels, a portion of the normal arbor is visible above the transverse nerve. Scale bar = 20 μm. (F) Quantification (mean ± SEM) of ectopic frequency in additional genotypes. As in MB γ neurons, the PlumBAC-GFP:HA transgene is able to completely rescue the *plum* mutant ectopic projection phenotype. Further, RNAi to *plum* only results in an ectopic connection phenotype when expressed in neurons, not muscles. In all cases, $n \geq 5$ larvae and 60 hemisegments scored. (G – H) The NMJ projecting to muscles 6 and 7 in a (G) control and (H) $plum^{\Delta 2}$ larva, stained with anti-HRP. No qualitative differences are evident in the normal arbor. Scale bar = 20 μm. (I) Quantification (mean ± SEM) of synaptic boutons in control (black bar) and $plum^{\Delta 2}$ (red bar) third instar larvae in segment A2. There are no statistically significant differences: Control = 103.5 ± 4.8 boutons, n = 24 NMJs, 12 larvae; $plum^{\Delta 2}$ = 123.6 ± 5.8 boutons, n = 23 NMJs, 12 larvae; $p > 0$.

Supplemental Experimental Procedures

Drosophila strains

Genotypes abbreviations: hsFlp is *y ,w ,hsFlp122*; CD8 is UAS-mCD8::GFP; mRFP is UAS-myr-mRFP; 40A, 2A and 82B are FRTs on 2L, 3L, and 3R, respectively; 201Y is 201Y-GAL4, OK107 is OK107-GAL4, elav is Elav-GAL4, Mef is DMef2-GAL4, Repo is Repo-GAL4, C155 is C155-GAL4, OK6 is OK6-GAL4; Gal80 is TubP-Gal80; UAS-*plum*^{RNAi} is UAS-*plum*-IR stock v101135 from the VDRC; UAS-*myo*^{RNAi} is UAS-*myo*-IR stock v102411 from the VDRC.

Figure 1: (B): hsFLP, CD8 / Y or +; 201Y, CD8 / + ; 82B, GAL80 / 82B. (C): hsFLP, CD8 / Y or + ; 201Y, CD8 / +; 82B, GAL80 / 82B, EMS$^{4-39}$, y+$^{@96E}$. (D): hsFLP, CD8 / Y or +; 201Y, CD8 / +; 82B, GAL80 / 82B, *plum*$^{\Delta 1}$. (E): hsFLP, CD8 / Y or +; 201Y, CD8 / UAS-*plum*^{wt}; 82B, GAL80/ 82B, *plum*$^{\Delta 1}$.

Figure 2: (A) hsFLP, CD8 / Y or +; CD8 / +; 82B, Gal80/ 82B; OK107. (B): hsFlp, CD8 / Y or +; CD8 / UAS-*plum*^{RNAi}; 82B, Gal80/ 82B, *plum*$^{\Delta 1}$; OK107/+.

Figure 3: (A): hsFlp, CD8 / Y or +; 201Y, CD8 / UAS-*plum*$^{\Delta Ig1-3}$*:Flag*; 82B, Gal80 / 82B, *plum*$^{\Delta 1}$. (B): hsFlp, CD8 / Y or +; 201Y, CD8 / UAS-*plum*$^{\Delta Ig1-4}$*:Flag*; 82B, Gal80 / 82B, *plum*$^{\Delta 1}$. (C): hsFlp, CD8 / Y or +; 201Y, CD8 / UAS-*plum*$^{\Delta Ig4}$*:Flag*; 82B, Gal80 / 82B, *plum*$^{\Delta 1}$. (D) hsFlp, CD8 / Y or +; 201Y, CD8 / UAS-*plum*$^{\Delta Cyt}$*:Flag*; 82B, Gal80 / 82B, *plum*$^{\Delta 1}$. (E) hsFlp, CD8 / Y or +; 201Y, CD8 / UAS-*plum*$^{ECD:m\text{CD8-}TM}$*:Flag*; 82B, Gal80 / 82B, *plum*$^{\Delta 1}$.

Figure 4: (A, B, C): 201Y, CD8. (D, E, F): 201Y, CD8; 82B, *plum*$^{\Delta 1}$ (G): UAS-*plum*^{RNAi} /+ ; *Actin5C-GAL4*/+ (H); C155/+; UAS-*plum*^{RNAi} /+ ; (I) UAS-*plum*^{RNAi} /+ ;Repo, CD8 /+ (J): hsFlp, CD8 / Y or +; Gal80, 40A, 201Y, CD8 / 40A; 82B, *plum*$^{\Delta 1}$. (K): hsFlp, CD8 / Y or +; Gal80, 40A, 201Y, CD8 / UAS-*plum*^{WT}*-HA*$^{29-1a}$ 40A; 82B, *plum*$^{\Delta 1}$ (L): hsFLP, CD8 / Y or +; 201Y, CD8 / UAS-*plum*^{wt}*:Flag*; 82B, GAL80/ 82B, *plum*$^{\Delta 1}$

Figure 5: (A): hsFlp, CD8 / Y or +; 201Y, CD8 / +; 82B, Gal80 / 82B. (B): hsFlp, CD8 / Y or +; 201Y, CD8 / +; 82B, Gal80 / 82B, *plum*$^{\Delta 1}$ (C): hsFlp, CD8 / Y or +; 201Y, CD8 / UAS-

plum^{WT}*:Flag*; 82B, Gal80 / 82B, *plum*$^{\Delta 1}$ (D): hsFlp, CD8 / Y or +; 201Y, CD8 / UAS-*plum*$^{\Delta Cyt}$*:Flag*; 82B, Gal80 / 82B, *plum*$^{\Delta 1}$ (E): hsFlp, CD8 / Y or +; 201Y, CD8 / +; 82B, Gal80 / 82B, *plum*$^{\Delta 1}$ (F) hsFlp, CD8 / Y or +; 201Y, CD8 / UAS-*EcR-B1*; 82B, Gal80 / 82B, *plum*$^{\Delta 1}$.

Figure 6: (A, B): hsFlp, CD8 / UAS-*Babo* ; 201Y, CD8 / +; 82B, Gal80 / 82B, *plum*$^{\Delta 1}$
(C, D): hsFlp, CD8 / Y or + ; 201Y, CD8 / UAS-*SmoX*$^{SDVD(10+12E)}$; 82B, Gal80 / 82B, *plum*$^{\Delta 1}$, (E, F): hsFlp, CD8/Y or +; UAS-*Plum*^{WT}*:Flag*, G13, *babo*^{52}/ G13, *G80*; *NP21-GAL4*/+ (G) UAS-*plum*$^{\Delta cyt}$*:Flag* / +; Repo/+, UAS-*plum*$^{\Delta cyt}$*:Flag* / +; Repo/ *plum*$^{\Delta 1}$, UAS- *plum*$^{\Delta cyt}$*:Flag* / +; Repo/ UAS-*myo*; (H) Repo/ UAS- *myo*, UAS-*plum*$^{\Delta cyt}$*:Flag* / +; Repo/ UAS- *myo*, UAS- *plum*$^{\Delta cyt}$*:Flag* / +; Repo, *plum*$^{\Delta 1}$*/ plum*$^{\Delta 1}$

Figure 7: (Control): *w; +;* 82B, 2A*; (plum*$^{\Delta 1}$*): w; +;* 82B, *plum*$^{\Delta 2}$*; (plum*$^{\Delta 2}$*): w; +;* 82B, *plum*$^{\Delta 2}$; (*plum*$^{\Delta 2}$ + Glia Plum^{WT}): *w;* UAS-*Plum*^{WT}*:HA* 40A / *+;* 82B, *plum*$^{\Delta 2}$, Repo*;* (*plum*$^{\Delta 2}$ + Muscle Plum^{WT}): *w;* Mef / UAS-*Plum*^{WT}*:HA* 40A*;* 82B, *plum*$^{\Delta 2}$; (*plum*$^{\Delta 2}$ + Nerve Plum^{WT}): *w;* elav / UAS-*Plum*^{WT}*:HA* 40A*;* 82B, *plum*$^{\Delta 2}$; (*plum*$^{\Delta 2}$ + Nerve Plum$^{\Delta Cyto}$): *w;* elav / UAS-*plum*$^{\Delta Cyt}$*:Flag;* 82B, *plum*$^{\Delta 2}$; (*plum*$^{\Delta 2}$ + Nerve Plum$^{\Delta Ig1-3}$): *w;* elav / UAS-*plum*$^{\Delta Ig1-3}$*:Flag;* 82B, *plum*$^{\Delta 2}$; (*plum*$^{\Delta 2}$ + Nerve Plum$^{\Delta Ig4}$): *w;* elav / UAS-*plum*$^{\Delta Ig4}$*:Flag;* 82B, *plum*$^{\Delta 2}$; (*babo*$^{32/52}$): *w*; *babo*$^{32/52}$; +; (Myo Nerve RNAi): w; elav / UAS-*myo*^{RNAi}; +; (Myo Muscle RNAi): w; Mef / UAS-*myo*^{RNAi}; +; (Motoneuron EcR DN): *w*; OK6 / UAS-*EcR.B1-ΔC655.F645A*; +; (*plum*$^{\Delta 1/\Delta 2}$ + Nerve EcR-B1): *w*; elav / UAS-*EcR-B1*; 82B, *plum*$^{\Delta 1}$ / 82B, *plum*$^{\Delta 2}$; (Nerve EcR-B1): *w*; elav / UAS-*EcR-B1*; +;

Figure S2: (A): UAS-*plum*^{FL}*/+;* CD8/+*;* OK107 (B): UAS-*plum*$^{\Delta Ig1-3}$*/+;* CD8/+*;* OK107 (C): UAS-*plum*$^{\Delta Ig1-4}$*/+;* CD8/+*;* OK107 (D): UAS-*plum*$^{\Delta Ig4}$*/+;* CD8/+*;* OK107 (E): UAS-*plum*$^{\Delta Cyt}$*/+;* CD8/+*;* OK107(F): UAS-*plum*$^{ECD:mCD8-TM}$*/+;* CD8/+*;* OK107.

Figure S3: (B, B') PlumBAC-GFP:HA/201y; UAS-mRFP/+

Figure S6: (A) yw; 201Y, CD8 (B) yw; 201Y, CD8; 82B, *plum*$^{\Delta 1}$

Figure S7**:** (Control): *w*; +; 82B, *2A*; (plum$^{\Delta 2}$): *w*; +; 82B, *plum$^{\Delta 2}$*; (plum$^{\Delta 2}$ + plum^{BAC}): *w*; *plumBAC-GFP:HA* / *CyO*; 82B, *plum$^{\Delta 2}$*; (Nerve plum RNAi): *w*; Elav / UAS-*plum^{RNAi}*; +; (Muscle plum RNAi): *w*; Mef / UAS-*plum^{RNAi}*; +

Construction of UAS-plum transgenes and transgenic flies

The full-length *plum* cDNA was cloned into pENTR-D/TOPO (Invitrogen) and verified by sequencing. Deletion of the various domains was performed by site directed mutagenesis (Finnzymes) using the pENTR-*plum* vector as a template. All deletion constructs were fully sequenced. Plum ORFs were recombined into Gateway based destination vectors by LR Clonase (Invitrogen). To allow site-specific integration of the transgene (Bischof et al., 2007), we used the gateway compatible plasmid pTWF-attB (Yaniv et al., 2012).

Deleted domains are (in amino acids): Ig1-3: 51-348, Ig 1-4: 51-451, Ig4: 356-451, Cytoplasmic domain: 937-END.

pUAS-PlumECD:mCD8-TM-Flag-AttB was created by deleting the transmembrane and cytoplasmic domains (907-END) in pENTR-*plum* and replacing them with the transmembrane domain of the mouse CD8 gene by blunt end ligation. The mCD8 TM domain was amplified using the following primers (5'-3'): GCCTGTGATATTTACATCTGGGC, GGATCCGCGGCTGTGGTAG.

Transgenes were injected by BestGene, Inc. or Genetic Services, Inc. All transgenes except those described in Figure 4K were injected into AttP40 using ϕC31-mediated integration. The transgene in Figure 4K was integrated using random P-element transgenesis, in which multiple flies were tested. The line UAS-plum^{WT}-HA$^{29\text{-}1a}$, inserted on chromosome 2, was chosen due to its high expression.

Plum antibody generation:

The Plum extracellular domain (Plum-ECD) followed by a C-terminal 3C protease site, an Fc tag, and a hexahistidine tag were all cloned into the baculoviral transfer vector pAcGP67A (BD Biosciences, Franklin Lakes, NJ). Baculoviruses were produced in Sf9 cells (*Spodoptera frugiperda*) by co-transfecting with the linearized baculoviral DNA Baculogold (BD Biosciences). Suspension cultures of High Five cells (*Trichoplusia ni*) in serum-free Insect-XPRESS medium (Lonza, Walkersville, MD) were infected with the Plum-ECD baculoviruses,

and culture media were collected 72 hours post-infection. Plum-ECD was purified either by immobilized metal affinity chromatography (IMAC) with Nickel-Nitrilotriacetic acid Agarose resin (QIAGEN), or by affinity to the Fc tag using Protein A Sepharose resin (Sigma-Aldrich). The Fc and hexahistidine tags were removed using human rhinovirus 3C protease, and undigested protein was removed with IMAC. Further purity was achieved with gel filtration chromatography using a Superose 6 column (GE Healthcare) in 10 mM HEPES pH 7.2 with 150 mM NaCl.

Purified Plum-ECD was injected into two New Zealand White rabbits at the Weizmann Institute Antibody Unit using an initial SQ injection and 3 IM boosts. Crude antisera from the exsanguination bleeds were then affinity purified using Plum-ECD coupled to CNBr-activated Sepharose 4 Fast Flow (Sigma-Aldrich). Purified fractions were eluted in 100 mM glycine, pH 2.5 and neutralized in 1 M Tris, pH 8. The affinity-purified antisera were then multiply preabsorbed against acetone-extracted protein powder made from third instar $plum^{\Delta 1}$ larvae, all according to established protocols (Harlow and Lane, 1988).

S2 aggregation assay

Vectors for the S2 aggregation assay were prepared by recombining the entry vectors described above using LR Clonase into the Gateway pAWG and pAWR destination vectors (*Drosophila* Gateway Collection, DGRC, Bloomington, IN). S2 cells were cultured at 25°C in Schneider's Drosophila Medium (Biological Industries) supplemented with 10% heat-inactivated FBS (Biological Industries). 5×10^6 cells in 5 ml were transfected with 3 µg of plasmid DNA using ESCORT IV (Sigma). Cells were pelleted 48 hr post-transfection and resuspended to a final concentration of approximately 1×10^6 /mL. Cells expressing $Plum^{WT}$:mRFP (1 mL) were mixed together with cells expressing a transgene tagged with GFP (1 mL) and transferred to a 35 mm well plate and supplemented with 2 mL of fresh Schneider's Drosophila Medium with 10% heat-inactivated FBS. Cells were then agitated at 90-RPM overnight at room temperature. Cells were left to settle for two hours without agitation and fixed using 4% PFA. GFP and RFP markers were visualized on a Zeiss 710 confocal microscope. An area of 7mm x 7mm was scanned and analyzed by MATLAB as follows:

We first analyzed the distribution of red aggregate size ($Plum^{WT}$:mRFP). The cell number in each aggregate was calculated by dividing each area by the average cell size (cell size was

calculated by averaging the area of single cells expressing cytoplasmic GFP and was set to ~80 μm^2). To avoid counting random cell interactions as aggregation, we set a minimum threshold of 5 cells as an aggregate. To calculate the percent of aggregates interacting with transgene-expressing cells, we calculated how many of the $Plum^{WT}$:mRFP aggregates overlapped with GFP-stained cells and divided by the total aggregates calculated above. To avoid counting random interactions with GFP expressing cells, we excluded aggregations of less than 3 cells.

REFERENCES:

Bischof, J., Maeda, R.K., Hediger, M., Karch, F., and Basler, K. (2007). An optimized transgenesis system for Drosophila using germ-line-specific phiC31 integrases. Proc Natl Acad Sci U S A *104*, 3312-3317.

Harlow, E., and Lane, D. (1988). Antibodies : a laboratory manual (Cold Spring Harbor, NY, Cold Spring Harbor Laboratory).

Venken, K.J., Carlson, J.W., Schulze, K.L., Pan, H., He, Y., Spokony, R., Wan, K.H., Koriabine, M., de Jong, P.J., White, K.P., *et al.* (2009). Versatile P[acman] BAC libraries for transgenesis studies in Drosophila melanogaster. Nat Methods *6*, 431-434.

Yaniv, S.P., Issman-Zecharya, N., Oren-Suissa, M., Podbilewicz, B., and Schuldiner, O. (2012). Axon regrowth during development and regeneration following injury share molecular mechanisms. Curr Biol *22*, 1774-1782.